BMC Cancer

RESEARCH

Open Access

Identification of a PANoptosis-related long noncoding rna risk signature for prognosis and immunology in colon adenocarcinoma

Yuekai Cui[1], Jie Mei[1], Shengsheng Zhao[1], Bingzi Zhu[1], Jianhua Lu[1], Hongzheng Li[1], Binglong Bai[1], Weijian Sun[2], Wenyu Jin[1], Xueqiong Zhu[1,3*], Shangrui Rao[1*] and Yongdong Yi[1*]

Abstract

Background PANoptosis, a complex programmed cell death (PCD) pathway that includes apoptosis, pyroptosis and necroptosis, is significantly involved in the progression of cancers. Long noncoding RNAs (lncRNAs) play crucial roles in PCD. However, the predictive value of PANoptosis-related lncRNAs (PRlncRNAs) for colon adenocarcinoma (COAD) has not been established.

Methods Gene expression data and clinical characteristics of patients with COAD were obtained from The Cancer Genome Atlas database. Differential expression analysis and Pearson correlation analysis were used to identify PRlncRNAs. In addition to least absolute shrinkage and selection operator, univariate and multivariate Cox regression analyses were employed to obtain PRlncRNAs for constructing a risk signature. Patients with COAD in the training set, testing set and entire set were stratified into high- and low-risk groups for further comparison of survival prognosis, using the median risk score as the cut-off point. Time-dependent receiver operating characteristic curves, a nomogram and multivariate Cox regression analysis were conducted to validate the risk signature in the testing set and the entire set. In addition, critical pathways, immune infiltration cells, immune checkpoint-related genes, Tumor Immune Dysfunction and Exclusion (TIDE) scores and antitumour drugs were compared between the two risk groups in the entire set. Correlations between ferroptosis, cuproptosis, disulfidptosis and the PRlncRNA risk score were evaluated. Finally, a competitive endogenous RNA (ceRNA) network was established, and enrichment analysis of the predicted mRNAs was performed using Gene Ontology (GO) analysis. The Kaplan–Meier plotter database was used as an external database to confirm the accuracy of the risk signature in predicting patient prognosis. Additionally, small interfering RNA (siRNA), a cell counting kit- 8 assay, a cell colony formation assay, quantitative polymerase chain reaction (qPCR) and an apoptosis assay were further employed to investigate the roles of AP003555.1 in colon cancer.

Results A risk signature comprising four PRlncRNAs (LINC01133, FOXD3-AS1, AP001066.1, and AP003555.1) was developed to predict the prognosis of patients with COAD. Kaplan–Meier curves demonstrated significant differences in prognosis between the high- and low-risk groups across the three sets. Multivariate Cox regression analysis confirmed that the risk signature was an independent prognostic factor across the three sets. A nomogram, receiver

*Correspondence:
Xueqiong Zhu
zjwzzxq@163.com
Shangrui Rao
rsr120@sina.com
Yongdong Yi
yiyongdong777@foxmail.com
Full list of author information is available at the end of the article

operating characteristic curves and calibration curves indicated strong confidence in the risk signature. Using the CIBERSORT algorithm and gene set enrichment analysis, variations in infiltrating immune cells and immune processes were observed between the two risk groups. Furthermore, TIDE algorithm suggested that the high-risk group exhibited a lower risk of immunotherapy escape and better immunotherapy outcomes than the low-risk group. Distinct responses to various antitumour drugs were observed between the two risk groups. Additionally, we constructed a ceRNA network based on PRlncRNAs, and GO enrichment analysis of the predicted mRNAs revealed different functions. In addition, the results of the Kaplan–Meier plotter database revealed that patients who exhibited high levels of LINC01133 and FOXD3-AS1 experienced significantly shorter overall survival than those with low levels of these lncRNAs. Specifically, in terms of functionality, AP003555.1 was found to be highly expressed in colon cancer tissue and promoted viability and proliferation while suppressing the apoptosis of colon cancer cells.

Conclusion We identified a novel risk signature consisting of four PRlncRNAs, which is an independent prognostic indicator for patients with COAD. This PRlncRNA risk signature is potentially relevant for immunotherapy and could serve as a therapeutic target for COAD.

Keywords PANoptosis, Long noncoding RNA, Risk signature, Colon adenocarcinoma

Introduction

Cancer accounts for 18% of all causes of death, second only to heart disease. Colorectal cancer (CRC) ranks as the second leading cause of cancer-related death globally [1]. The global CRC incidence rate is estimated to more than double by 2035 and may be associated with risk factors, such as personal and medical history, family history and lifestyle factors [2]. Colon adenocarcinoma (COAD) is the most prevalent subtype of CRC. In recent years, the mortality rate of COAD has exhibited a declining trend, attributed to the rapid advancement of early screening techniques and the availability of diverse therapeutic interventions [3–5]. However, only 40% of cases can be detected in the early tumour stage, and postoperative recurrence and chemotherapy resistance increase the risk of therapeutic failure [6]. Overall, the prognosis of patients with late-stage COAD remains poor. Hence, there is an urgent need for a reliable risk assessment model to complement and enhance traditional risk stratification methods. This model could aid in identifying patients with COAD with a poor prognosis more accurately.

The advancement of next-generation sequencing technology has led to extensive research on long noncoding RNAs (lncRNAs), which are transcripts exceeding 200 nucleotides in length and lacking protein coding potential [7]. Numerous previous studies have revealed that dysregulated lncRNAs may be new prognostic and diagnostic biomarkers in COAD [8, 9]. The lncRNAs ALMS1-IT1 and IGFL2-AS1 are positively correlated with poor overall survival in patients with COAD [10, 11]. In addition, many prognostic risk models based on lncRNAs, such as angiogenesis-related lncRNAs [12] and disulfidptosis-related lncRNAs, have been established [13]. The competitive endogenous RNA (ceRNA) network, proposed by Salmena and colleagues, revealed a novel mechanism of RNA interactions across various cancers [14]. The lncRNAs can affect the prognosis of patients with COAD and progression of colon cancer through different ceRNA networks [15–19]. These findings suggest the possibility of developing more precise prognostic biomarkers using lncRNAs and constructing prognostic risk models for patients with COAD.

Programmed cell death (PCD) is pivotal for maintaining homeostasis within an organism, and three key PCD pathways have been extensively studied: apoptosis [20], pyroptosis [21] and necroptosis [22]. Increasing evidence suggests diverse significant cross-talks among these three pathways. Professor Kanneganti's team introduced PANoptosis as an inflammatory PCD pathway activated by specific triggers and regulated by PANoptosome complexes. PANoptosis is a key characteristic of pyroptosis, apoptosis and necroptosis but cannot be explained solely by any of these three PCD pathways [23]. Wang et al. developed a PANoptosis-based molecular clustering and prognostic signature that is crucial for predicting survival outcomes in patients with COAD [24]. Furthermore, Huang et al. pinpointed lncRNA-SNHG7 as a potential target linked to PANoptosis and metastasis in COAD [25]. However, there remains a gap in understanding the biological functions of PRlncRNAs and the clinical significance of prognostic risk models in COAD.

In our study, as shown in Fig. 1, we established a novel PRlncRNA risk signature using data from The Cancer Genome Atlas (TCGA) database. We systematically assessed the prognostic significance of this risk signature and its correlation with clinicopathological characteristics among patients with COAD. We subsequently developed a nomogram to increase the accuracy of prognosis prediction for patients with COAD, thereby improving individualized prediction efficiency. Furthermore, we evaluated immune cell infiltration, as

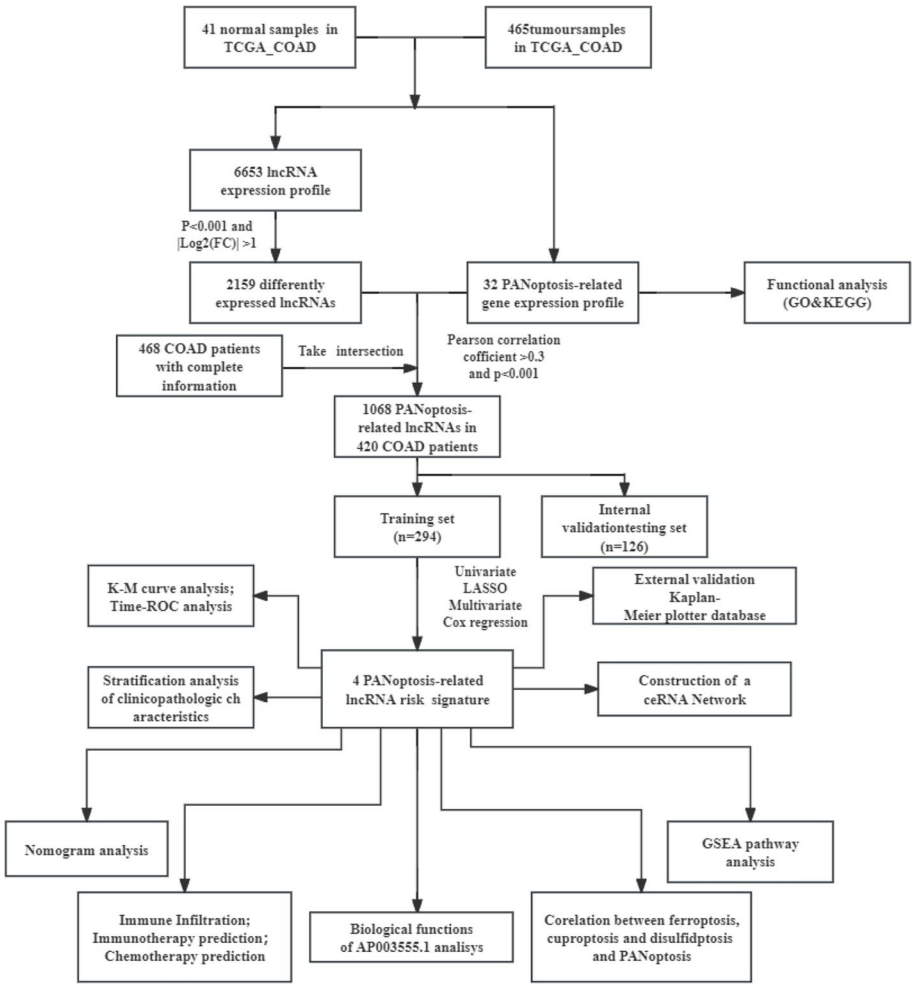

Fig. 1 Flowchart of the study process

well as the response to both immunotherapy and antitumour drugs, between the two risk groups. Additionally, we examined the correlations between ferroptosis, cuproptosis, disulfidptosis and the PRlncRNA risk score. We found that patients who exhibited elevated levels of LINC01133 and FOXD3-AS1 experienced significantly shorter overall survival and recurrence-free survival than patients with reduced levels of these lncRNAs. Finally, we constructed a ceRNA network and identified AP003555.1 as a promoter of viability and proliferation while suppressing the apoptosis of colon cancer cells. Overall, our study established a prognostic risk model associated with PRlncRNAs and their potential regulatory mechanisms, which may enhance prognostic assessments and personalized treatments in patients with COAD.

Materials and methods

Downloading and processing of the COAD patient dataset

We obtained count and fragments per kilobase of transcript per million reads mapped (FPKM) data for 506 COAD samples (comprising 465 tumour samples and 41 normal samples) from the TCGA dataset (https://portal.gdc.cancer.gov/). The data of 420 eligible patients with COAD with overall survival (OS) times greater than 0 days and complete individual clinical information were downloaded. The survival information and clinical characteristics are listed in Additional Table 1.

Functional enrichment analysis of PANoptosis-related genes

Previous studies have identified 32 PANoptosis-related genes (PRGs) from the literature [26, 27]. Using

the"ClusterProfiler"package (version 4.8.2), functional enrichment analysis was conducted to identify Gene Ontology (GO) terms and Kyoto Encyclopedia of Genes and Genomes (KEGG) pathways associated with these 32 PRGs. The results were visualized and plotted using the"ggplot2"package (version 3.4.3).

Identification of PANoptosis-related LncRNAs in COAD

Differential expression analysis of lncRNAs between tumour and normal samples was conducted via the"DESeq2"package (version 1.40.2). LncRNAs with a | log2 (fold change) |> 1.0 and a p value < 0.05 were considered differentially expressed and visualized via the"pheatmap"package (version 1.0.12). To identify PRlncRNAs, Pearson correlation analysis was performed to assess the correlation between PRGs and differentially expressed lncRNAs. The criteria for selecting PRlncRNAs were a Pearson correlation coefficient > 0.3 and a p value < 0.001.

Random grouping of patients with COAD

The 420 eligible patients with COAD were randomly divided into two sets: a training set comprising 70% of the samples and a testing set comprising 30% of the samples. This random partitioning was performed via the"caret"package (version 6.0.94).

Establishment and validation of a PANoptosis-related LncRNA risk signature

Univariate Cox regression analysis (p < 0.05) was employed to identify PRlncRNAs significantly associated with survival in the training set. Subsequently, least absolute shrinkage and selection operator (LASSO) and multivariate Cox regression analyses (p < 0.05) were conducted to construct a PRlncRNA risk signature. This risk signature was then validated in the testing set and the entire set.

The risk score for each individual COAD patient was calculated via the following formula: Σcoefficient of (PRlncRNAi) ×expression of (PRlncRNAi). In the training set, patients with COAD were stratified into high- and low-risk groups based on the median risk score. Similarly, risk scores were computed for all patients with COAD in both the testing set and the entire set. These patients were subsequently divided into high- and low-risk groups on the basis of the same median point as determined in the training set. Kaplan–Meier survival analyses were conducted to compare the survival probability between the high- and low-risk groups in all three sets via the"survminer"(version 0.4.9) and"survival"packages (version 3.5.7). A significance level of p < 0.05 was considered statistically significant. Time-dependent receiver operating characteristic (ROC) curves and area under the curve (AUC) values were established to evaluate the predictive accuracy and specificity of the risk score system, as were significant clinicopathological characteristics such as age, sex and tumour stage. This was accomplished via the"timeROC"package (version 0.40) for the risk signature and the"pROC"package (version 1.0.11) for age, sex and tumour stage.

Construction and calibration of a predictive nomogram

Using the"rms"package (version 6.7.1), a nomogram was constructed that incorporates the PRlncRNA risk score along with clinicopathologic characteristics such as sex, age, and tumour stage to predict the 1-, 3-, and 5-year survival rates of patients with COAD. ROC curves were subsequently generated to assess the prediction accuracy of the nomogram, and the discrimination ability was subsequently examined based on the degree of fit of the calibration curves.

Functional gene set enrichment analysis (GSEA)

The"ClusterProfiler"package was utilized to investigate critical pathways in biological processes associated with the PRlncRNA risk signature across different subgroups in the entire set. The gene sets"c2.cp.kegg.v7.4.symbols"and"c7.all.v7.4.symbols"(immunologic signatures) were obtained from the MSigDB database (https://www.gsea-msigdb.org/gsea/msigdb) for GSEA. A significance threshold of p < 0.05 was applied to determine statistical significance.

Analysis of tumour-infiltrating immune cells

To compare the immune infiltration levels between the high- and low-risk groups in the entire set, the CIBERSORT algorithm was used to estimate the abundance of infiltrating immune cells. Additionally, given the potential association between the prediction efficiency of immune checkpoint inhibitors and the expression of immune checkpoint-related genes, the relationships between immune checkpoint genes and the PRlncRNA score were analysed to investigate the potential roles of the PRlncRNA risk signature.

Response to immunotherapy and antitumour drugs

The potential response of patients with COAD to immunotherapy was predicted via the Tumor Immune Dysfunction and Exclusion (TIDE) (http://tide.dfci.harvard.edu/) algorithm. Additionally, the half inhibitory concentration (IC50) of each sample was estimated for assessing antitumour drugs by using the"oncoPredict"package (version 0.2). A lower IC50 value indicates greater sensitivity to drugs.

Correlations between ferroptosis, cuproptosis, and disulfidptosis and the PANoptosis-related lncRNA risk score

The correlations between the PRlncRNA risk score and the enrichment score (ES) of ferroptosis, cuproptosis and disulfidptosis were examined using the gene set variation analysis (GSVA) method with the"GSVA"package (version 1.48.4). Pearson correlation analysis was conducted to analyse these relationships. Genes related to ferroptosis were obtained from the FerrDb database (http://www.zhounan.org/ferrdb/current/), while cuproptosis-related genes [28, 29] and disulfidptosis-related genes [30–33] were identified from previous literature.

Establishment and analysis of a CeRNA network

Initially, the target microRNAs (miRNAs) of the PRlncRNAs were retrieved from the DIANA-LncBase v3 database, and the corresponding target mRNAs of these miRNAs were selected from the Encyclopaedia of RNA Interactomes (ENCORI) database. Subsequently, Pearson correlation analysis was conducted to assess the relationships among PRlncRNAs, miRNAs and mRNAs. Finally, the lncRNA–miRNA–mRNA regulatory relationships were integrated to construct a ceRNA network via Cytoscape. Additionally, GO enrichment analysis was employed to identify the potential functions of the identified PRlncRNAs.

External dataset validation

The Kaplan–Meier plotter database was used as an external database to predict OS and recurrence-free survival (RFS) in patients with different levels of PRlncRNA expression.

RNA extraction and quantitative polymerase chain reaction (qPCR)

Eight paired tumour and paratumour colon cancer tissue samples were acquired from The 2nd Affiliated Hospital and Yuying Children's Hospital of Wenzhou Medical University. The survival information and clinical characteristics are listed in Additional Table 2. Our study was approved by the Ethical Committee of The 2nd Affiliated Hospital and Yuying Children's Hospital of Wenzhou Medical University (Approval Number: 2023-K- 247–02). Colon cancer tissue (1 mm^3) was removed and homogenized via a homogenizer (16,073,403, MP Biomedicals, California, USA). One ml of the total RNA extraction reagent TRIzol (15,596,026; Thermo Fisher Scientific, Shanghai, China) was added, and the mixture was incubated on ice for 10 min. After the first centrifugation, the upper clear liquid was transferred to a new Eppendorf tube, and 200 µl of chloroform was added individually. The mixtures were vigorously shaken for 15 s and incubated at room temperature for 5 min. After the second centrifugation, the upper aqueous phase was transferred to a new Eppendorf tube, and 600 µl of isopropanol was added individually. The mixtures were mixed 10 times and left at room temperature for 10 min. After the third centrifugation, the supernatant was removed, and the RNA precipitate was washed twice with 1 ml of 75% ethanol. After the fourth centrifugation, the supernatants were removed and air dried at room temperature for 25 min. The obtained RNA was dissolved in 30 µl of diethyl polycarbonate water. The obtained RNA was subsequently reverse transcribed into cDNA via HiScript II reverse transcriptase (Vazyme, Nanjing, China). The qPCR assays were performed via ChamQ SYBR Colour qPCR Master Mix (Q411; Vazyme Biotech, Nanjing, China) in a 96-well plate. Finally, the expression levels were calculated via the 2- ΔΔCT method. Actin was used as a standard control, and the primers used for amplifying AP003555.1 and actin were procured from Sangon Biotech (Shanghai, China). The sequences are listed in Additional Table 3.

Cell culture and small interfering RNAs (siRNAs) treatment

The human colon cell lines LoVo and SW480 were procured from the National Collection of Authenticated Cell Cultures (Shanghai, China). LoVo and SW480 cells were cultured in T25 cell culture flasks in complete Roswell Park Memorial Institute (RPMI)– 1640 medium (Gibco, California, USA) containing 5% foetal bovine serum and 1% penicillin–streptomycin solution and were maintained at 37 °C in a constant-temperature incubator with 5% CO_2. LoVo and SW480 cells were seeded into 6-well cell culture plates at 50–60% confluence and transfected after 24 h. Silencing RNA that affected AP003555.1 was synthesized by Hangzhou Repobio (Hangzhou, China).

SiRNAs that silence ATP1 A1 were transfected into cells using Lipofectamine 3000 Reagent (Thermo Fisher, Shanghai, China) according to the manufacturer's instructions. The knockdown efficacy was assessed using qPCR 48 h after transfection as described above, and after transfection, the cells were harvested for subsequent functional assays.

Cell Counting Kit- 8 (CCK- 8)

The human colon cell lines LoVo and SW480 were individually seeded in a 96-well plate at a density of 1.5 × 104 cells per well and incubated with 100 µL of complete culture medium for 24 h. Subsequently, gradient concentrations of oxaliplatin (0, 5, 10, 15, 25, 30, and 35 µm) were individually added to a 96-well plate and further cultured for 24 h. Finally, 10 µL of CCK- 8 reagent was added to each well, and the mixture was incubated the 96-well plate for 60 min. The optical density value was

determined at a wavelength of 450 nm via a microplate reader (1,110,007,004, Tecan, Mannedorf, Switzerland). The absorbance at 450 nm was indicative of the growth rate of cells.

Cell colony formation

The human colon cell lines LoVo and SW480 were seeded into a 12-well plate at 700 cells per well and cultured for 7 days at 37 °C with 5% CO_2 to allow colony formation. Lovo cells were treated with 0, 15, or 30 μm oxaliplatin, and SW480 cells were treated with 0, 5, or 10 μm oxaliplatin for 48 h. Following incubation, the colonies were fixed with 4% paraformaldehyde for 15 min and then stained with 0.1% crystal violet for an additional 20 min. The plates were subsequently washed with flowing water to remove excess dye and allow the formation of distinct cell colonies. Finally, photos of the plate were acquired, and the results were analysed using ImageJ software.

Apoptosis assay

The cells were divided into two groups, the negative control (NC) group and the si-AP003555.1 group, at a density of 1.5 ×104 cells per well in 6-well plates. Lovo cells were treated with 0, 10, or 20 μm oxaliplatin, and SW480 cells were treated with 0, 15, or 30 μm oxaliplatin for 24 h. To collect the cells, the supernatant from a 6-well plate was first collected. The cells were then washed once with phosphate-buffered saline (PBS) and collected using 500 μL of trypsin. After thorough mixing, the cell suspension was centrifuged at 4 °C for 5 min to collect the cells. The cells were subsequently washed again with PBS. Next, the cells were incubated at room temperature in the dark with the membrane-associated proteins Annexin V-FITC and propidium iodide (PI) for 20 min. The plates were then immediately analysed using Beckman Coulter flow cytometry. The data collected were analysed using FlowJo v10 software.

Statistical analysis

Statistical analyses were performed using R software (version 4.3.1). Kaplan–Meier curves were used to visualize differences in survival probability, and the log-rank test was used to compare survival disparities. Univariate and multivariate Cox analyses were conducted using the"survival"package. LASSO Cox regression analysis was performed using the"glmnet"package (version 4.1.8). The experimental data were processed using Prism 8 software. The Student's t test was used to determine the statistical significance of differences between independent groups for continuous variables, which are presented as the standard error of the mean. Categorical data were compared using the chi-square test. Statistical significance was considered at $p < 0.05$ and indicated as $^{*}P < 0.05$, $^{**}P < 0.01$, and $^{***}P < 0.001$.

Results

Functional enrichment analyses of PANoptosis-related genes

We acquired and presented 32 PRGs from previous literature, which are listed in Additional Table 4. Functional enrichment analyses were subsequently conducted to identify related GO terms and KEGG signalling pathways. According to the GO functional enrichment analysis, the PRGs were enriched mainly in biological processes, such as PCD ($P = 8.50E-22$), necroptotic processes ($P = 4.02E-17$), apoptotic processes ($P = 4.61E-19$), pyroptosis ($P = 1.88E-27$) and regulation of the immune response ($P = 2.27E-19$). Molecular function revealed that the PRGs were related to cysteine-type endopeptidase activity involved in apoptotic processes ($P = 1.56E-14$) and tumour necrosis factor receptor binding ($P = 2.01E-07$) (Fig. 2A). The KEGG functional enrichment analysis revealed that the PRGs were associated with necroptosis ($P = 1.01E-16$), apoptosis ($P = 9.35E-10$) and the MAPK signalling pathway ($P = 0.024$) (Fig. 2B).

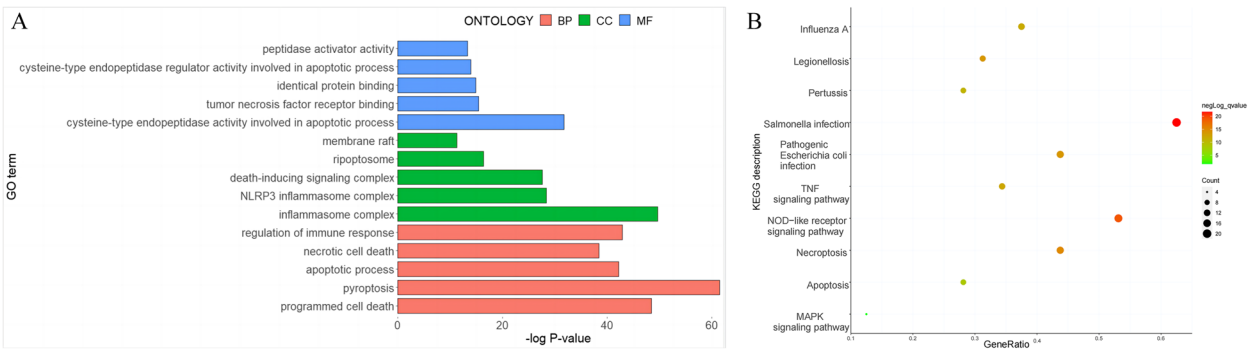

Fig. 2 Functional enrichment analyses of PANoptosis-related genes. **A** Gene Ontology functional enrichment analysis. **B** Kyoto Encyclopedia of Genes and Genomes functional enrichment analysis

Construction of the PANoptosis-related lncRNA risk signature in COAD

We identified 2159 differentially expressed lncRNAs between normal and tumour samples (| log2 (fold change) |> 1 and p value < 0.05). A volcano plot depicting these findings is provided in Additional Fig. 1. Subsequently, 1086 PANoptosis-related differentially expressed lncRNAs were identified through Pearson correlation analysis (Pearson's coefficient > 0.3 and p < 0.001) (Additional Table 5). Next, 420 eligible patients with COAD were randomly allocated into two sets: a training set comprising 70% of the entire set (n = 294 patients) and a testing set comprising 30% of the entire set (n = 126 patients). Table 1 displays the clinical features of the patients with COAD after grouping.

Subsequently, univariate Cox regression analysis was conducted to identify PRlncRNAs associated with OS time in the training set. This analysis led to the identification of 103 PRlncRNAs, as detailed in Additional Table 6. Furthermore, LASSO Cox regression analysis was employed to construct a risk model containing 43 PRlncRNAs. The selection of these PRlncRNAs occurred when the partial likelihood deviation reached its minimum, with an optimal log (lambda) value of − 3.730, as illustrated in Fig. 3A and B. In the final step, multivariate Cox regression analysis identified four significant PRlncRNAs (LINC01133, FOXD3-AS1, AP001066.1, and AP003555.1) for constructing a risk signature (Fig. 3C, Table 2). The coefficients of all four PRlncRNAs were positive, indicating that they were risk factors. A Sankey diagram shows the associations between PRGs and PRlncRNAs (Fig. 3D).

A PRlncRNA risk signature for patients with COAD was established by integrating the regression coefficients and expression values of four PRlncRNAs. The risk score was calculated as follows: risk score = 0.5498 × expression value of LINC01133 + 1.6440 × expression value of FOXD3-AS1 + 1.0300 × expression value of AP001066.1 + 0.0291 × expression value of AP003555.1. According to the median point of − 0.1131631, the patients with COADpatients with COAD in the training set were stratified into high- and low-risk groups. Kaplan–Meier curve analysis revealed that patients with COAD in the high-risk group exhibited poorer survival compared with that in the low-risk group, as depicted in Fig. 4A, B shows that as the risk score increased, the survival status and distribution of patients decreased, whereas the expression levels of the four PRlncRNAs increased. An identical risk score formula was applied to both the testing set and the entire set. Patients with patients with COADwere stratified into high- and low-risk groups based on the same median score. The results were similar to those in the testing set and the entire set (Fig. 4D, E, G, H. The AUC values for the PRlncRNA risk signature generated by time–ROC analysis in the training set were 0.768, 0.782, and 0.714 for 1-, 3-, and 5-year survival, respectively (Fig. 4C), and the corresponding AUC values were 0.609, 0.685, and 0.736 in the testing set (Fig. 4F) and 0.720, 0.750, and 0.708 in the entire set, respectively (Fig. 4I). These results underscore the robust predictive ability of the risk score system.

Table 1 Clinical features of the patients with COAD with COAD in the two sets

Group	Testing set	Training set	P
	***N* = 126**	***N* = 294**	
Status, n (%)			0.131
Alive	93 (73.8)	238 (81.0)	
Dead	33 (26.2)	56 (19.0)	
Gender, n (%)			0.088
Female	67 (53.2)	128 (43.5)	
Male	59 (46.8)	166 (56.5)	
Age (years), Mean (SD)	65.3 (13.8)	67.0 (12.4)	0.213
Tumour Stage, n (%)			0.188
I	17 (13.5)	56 (19.0)	
II	54 (42.9)	112 (38.1)	
III	32 (25.4)	89 (30.3)	
IV	23 (18.3)	37 (12.6)	

Associations between the PRlncRNA risk signature and the clinicopathologic characteristics of patients with COAD with COAD

To confirm the predictive efficacy of the PRlncRNA risk signature in combination with clinicopathologic variables such as age, sex, and tumour stage in patients with COAD, univariate and multivariate Cox regression analyses were conducted on three sets (training, testing, and entire sets). These analyses are summarized in Table 3. According to the univariate Cox regression analysis of the training set, the risk signature, tumour stage, and age were significantly correlated with OS in patients with COAD. Subsequent multivariate Cox regression analysis utilising these three clinicopathologic variables confirmed that the risk signature was an independent factor. These findings were further validated in both the testing and entire sets. The relationships between the PRlncRNA risk signature and clinicopathological characteristics were subsequently examined in the entire set. The strip chart analysis revealed significant disparities between the high- and low-risk groups concerning survival status and tumour stage, as depicted in Fig. 5A. Moreover, ROC curves were generated to evaluate the accuracy of the significant clinicopathological variables within the risk score system. The AUC values for the PRlncRNA

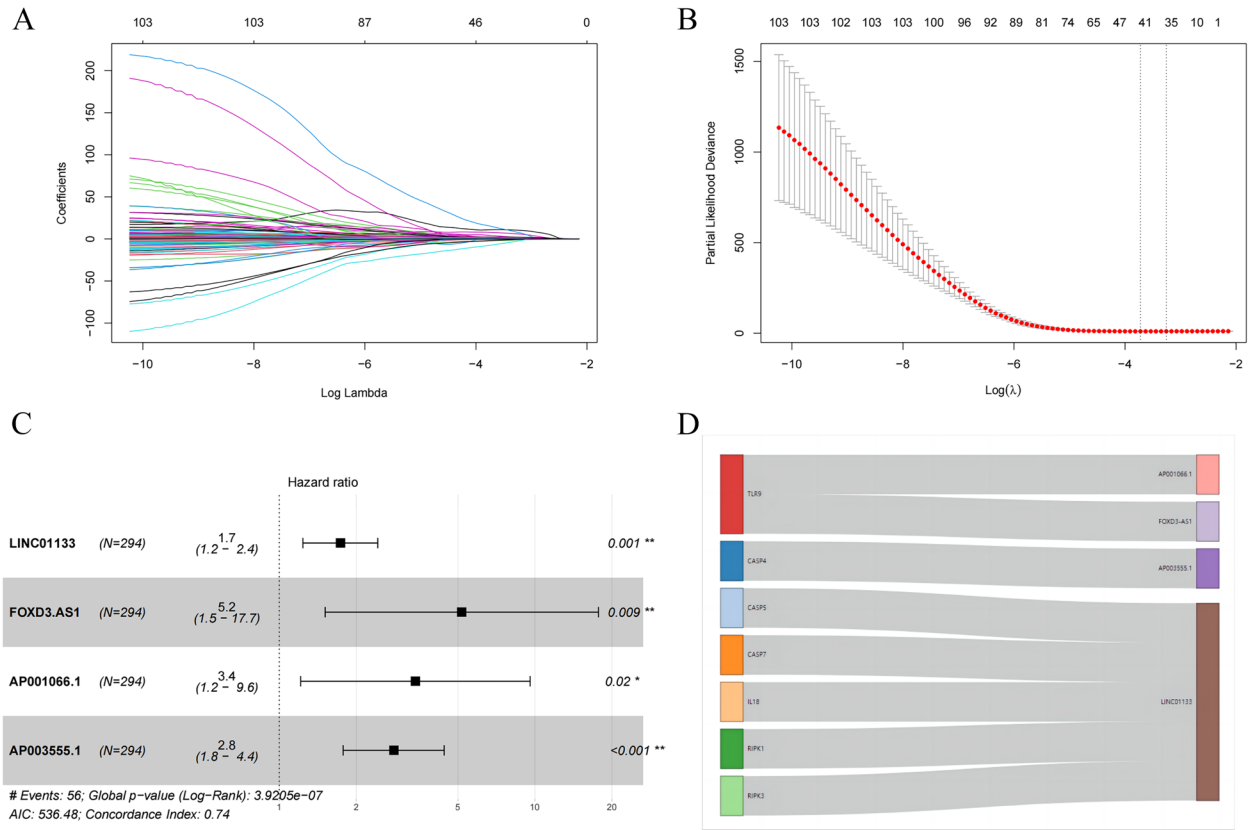

Fig. 3 Construction of the PANoptosis-related lncRNA risk signature for patients with COAD in the training set. **A**, **B** LASSO Cox regression analysis and partial likelihood deviance for evaluating prognostic PRlncRNAs. **C** Four PRlncRNAs identified by multivariate Cox regression analysis for constructing a risk score system. **D** Sankey diagram of the correlation between PRlncRNAs and PRGs

Table 2 Multivariate Cox regression analysis of four prognostic PRlncRNAs

PRlncRNAs	Coefficient	HR	CI (95%)	*P* value
LINC01133	0.5498	1.7328	1.237–2.428	0.0014
FOXD3-AS1	1.6440	5.1757	1.512–17.719	0.0089
AP001066.1	1.2259	3.4073	1.213–9.574	0.0200
AP003555.1	1.0300	2.8012	1.777–4.415	9.1e- 06

risk score, tumour stage, age and sex were 0.669, 0.700, 0.579 and 0.5094, respectively (Fig. 5B). Additionally, patients with COAD were stratified based on age, sex, and tumour stage. Notably, patients in the high-risk subgroup had significantly poorer prognoses across all subgroups, including the early tumour stage subgroup (stage I_II) (Fig. 5C) and late tumour stage subgroup (stage III_IV) (Fig. 5D), as well as across sex (female and male) (Fig. 5E, F) and age subgroups (≤ 60 years and > 60 years) (Fig. 5G, H), than those in the low-risk subgroup. Taken together, these findings revealed the robust performance of the PRlncRNA risk signature in predicting OS among patients with COAD.

Construction and evaluation of a prognostic nomogram

A nomogram was developed to predict the 1-, 3-, and 5-year OS probabilities of patients with COAD in the training set. The nomogram integrated the PRlncRNA risk score and clinicopathologic variables such as age, sex, and tumour stage, enhancing the clinical applicability of the risk model (Fig. 6A). The estimated AUC values of the ROC curves for 1-, 3-, and 5-year survival were 0.840, 0.873, and 0.748, respectively, in the training set (Fig. 6B). Similarly, in the testing set, the AUC values for 1-, 3-, and 5-year survival were 0.792, 0.833, and 0.894, respectively (Fig. 6C). In the entire set the AUC values for 1-, 3-, and 5-year survival were 0.825, 0.864, and 0.796, respectively (Fig. 6D). Moreover, good concordance between the observed and predicted 1-, 3-, and 5-year OS rates in the three sets was found, as shown in the calibration plots (Fig. 6E, F, G). Overall, these findings indicated that the nomogram had a good ability to predict the survival probability of patients with COAD with COAD.

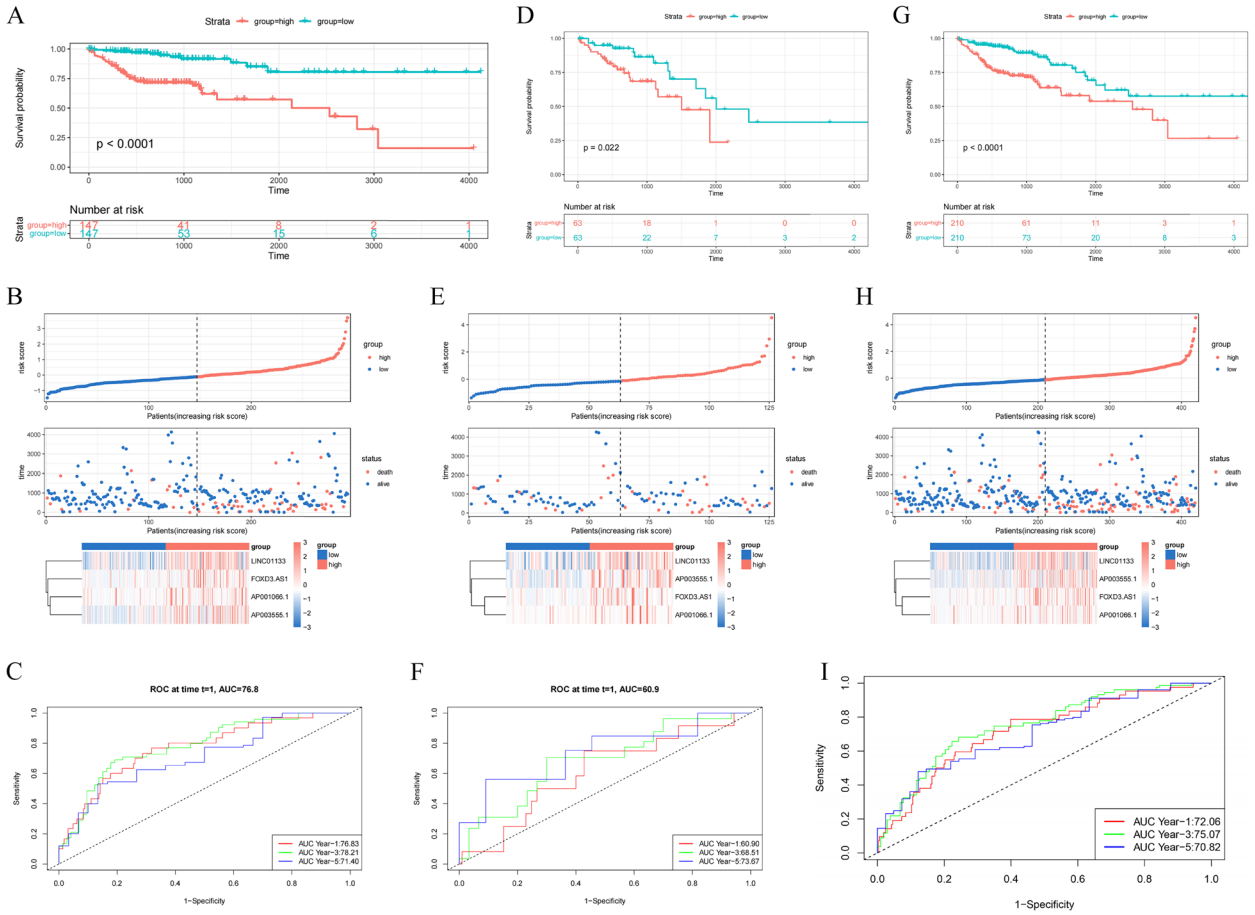

Fig. 4 Prognostic evaluation and validation of the PANoptosis-related lncRNA risk signature for overall survival in patients with COAD across the three sets. K–M survival curves in the training set (**A**), testing set (**D**) and entire set (**G**). The risk score, survival status and heatmaps of the expression of the four lncRNAs between the high- and low-risk groups are shown for the training set (**B**), testing set (**E**), and entire set (**H**). The AUC values of the ROC curves in the training set (**C**), testing set (**F**), and entire set (**I**)

Identification of pathways related to the PRlncRNA risk signature

To identify the pathways associated with the risk score, we conducted GSEA to investigate the potential differences in biological processes and pathways between the high- and low-risk groups. Ascorbate and aldarate metabolism, pentose and glucuronate interconversions, steroid hormone biosynthesis, retinol metabolism and metabolism of xenobiotics by cytochrome P450 were enriched in the high-risk group, whereas DNA replication, mismatch repair, ribosome RNA polymerase and aminoacyl-tRNA biosynthesis were significantly enriched in the low-risk group (Fig. 7A). These findings suggested that the pathways enriched in the high-risk group were associated with metabolic processes.

Furthermore, we observed a significant association between the high-risk group and several immune processes, including GSE10325_CD4_TCELL_VS_BCELL_DN, GSE13887_ACT_CD4_VS_NO_TREATED_CD4_TCELL_UP, GSE29618_BCELL_VS_PDC_UP, GSE29618_BCELL_VS_MDC_UP and GSE40666_STAT1_KO_VS_STAT4_KO_CD8_TCELL_DN (Fig. 7B). These results indicate that the PRlncRNA risk signature may be associated with the tumour immune microenvironment.

Association of the PRlncRNA risk signature with immune infiltration and therapeutic effects

To further explore the connection between the PRlncRNA risk signature and tumour-infiltrating immune cells, we utilized the CIBERSORT algorithm to assess the differences in immune infiltration between the low- and high-risk groups. Figure 8A shows that patients with COAD in the high-risk group exhibited lower levels of infiltrating macrophages and activated mast cells but greater levels of regulatory T cells and $CD8^+$ T cells than those in the low-risk group. These findings suggested significant differences in the tumour

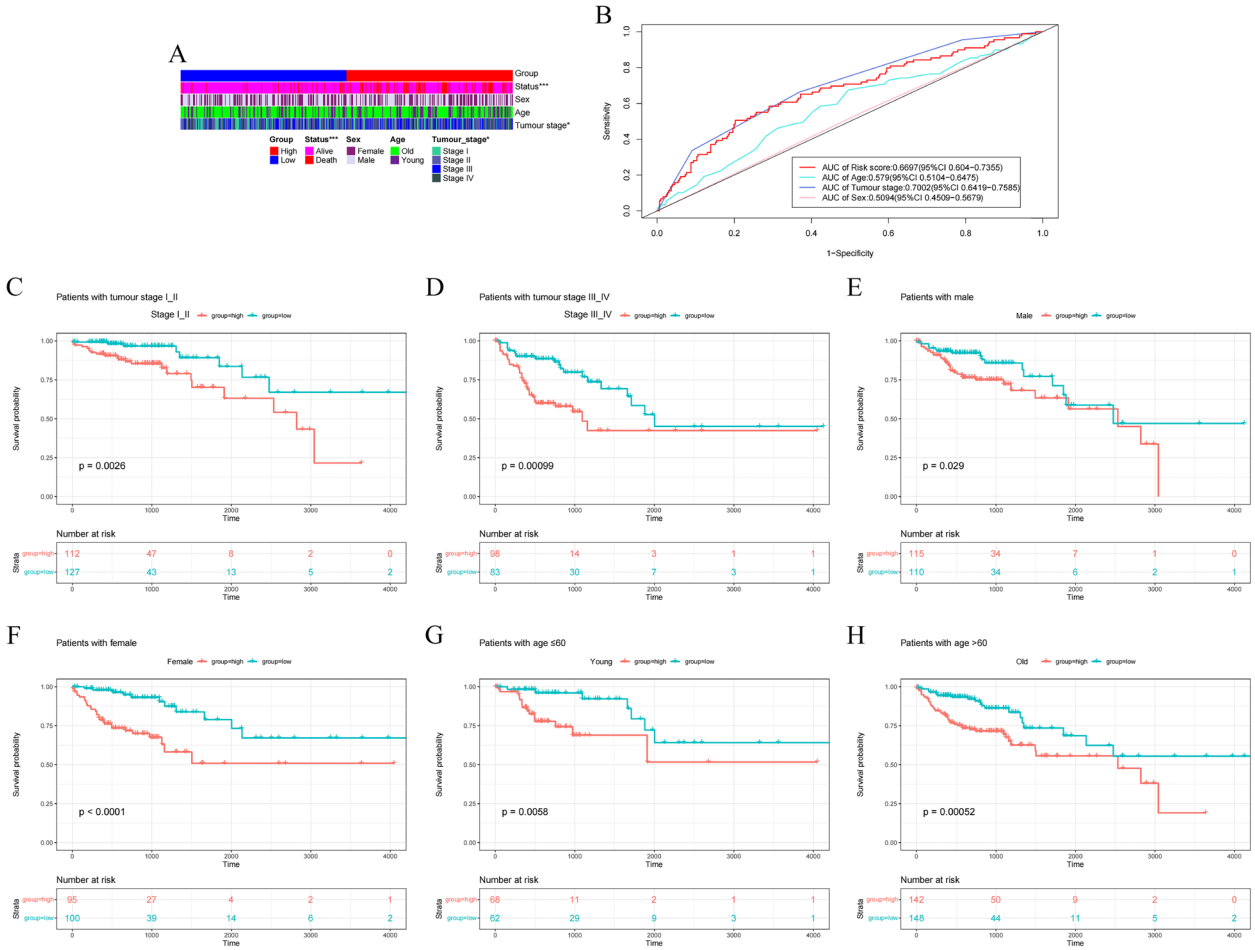

Fig. 5 Correlations between the PANoptosis-related lncRNA risk signature and clinicopathological characteristics of patients with COAD across the entire set. **A** Strip chart displaying the relationships between clinical characteristics across the two groups. **B** The AUC values of the ROC curves comparing the predictive accuracy of the risk score and other prognostic variables. Clinical stratification analysis of OS in patients with COAD across the two groups stratified by tumour stage (**C**, **D**), sex (**E**, **F**) and age (**G**, **H**)

immune microenvironment between the low- and high-risk groups. Figure 8B shows that three genes (BTLA, HHLA2, and IDO2) were highly expressed in the high-risk group, which was particularly relevant in the context of checkpoint-based immunotherapy. The patients in the high-risk group exhibited markedly lower TIDE scores than the low-risk group, indicating a potential association between the risk signature and immunotherapy response (Fig. 8C).

Figure 8D shows that the high-risk group had lower IC50 values for afatinib, sapitinib, acetalax, and buparlisib than the low-risk group, suggesting potential differences in antitumour drugs between the two risk groups.

Correlations among ferroptosis, cuproptosis, disulfidptosis and the PRlncRNA risk signature

The GSEA revealed significant enrichment of ferroptosis genes in the low-risk group (Fig. 9A). Thus, 485 ferroptosis-related genes were extracted from the FerrDb database, and the associations between the risk score and the ES of ferroptosis were explored. The results revealed that these variables were negatively correlated ($R = -0.112$ and $p = 0.021$) (Fig. 9B). As novel modes of PCD, cuproptosis and disulfidptosis have been widely studied. Moreover, we identified 19 genes related to cuproptosis and 26 related to disulfidptosis from previous studies (Additional Table 7). The relationship between the ES of cuproptosis and the risk score was similar to that between the ES of ferroptosis and the risk score ($R = -0.15$ and $p = 0.002$) (Fig. 9C). However, no significant difference was observed between the ES of disulfidptosis and the risk score (Fig. 9D).

Table 3 Univariate and multivariate Cox regression analyses of the PRlncRNA risk signature and clinicopathologic characteristics in the three sets

Clinicopathologic Characteristics	Univariable			Multivariable		
	HR	HR (95%)	*P* value	HR	HR (95%)	*P* value
Training set						
Age	1.03	1–1.05	0.037	1.03	1.01–1.06	0.010
Gender	1.07	0.63–1.82	0.803			
Tumour stage	1.86	1.38–2.51	< 0.001	2.19	1.58–3.06	< 0.001
Risk signature	2.72	2.04–3.62	< 0.001	2.78	2.09–3.71	< 0.001
Testing set						
Age	1.01	0.98–1.04	0.47			
Gender	1.25	0.63–2.5	0.521			
Tumour stage	3.05	2.01–4.62	< 0.001	3.16	2.04–4.89	< 0.001
Risk signature	1.46	1.06–2.02	< 0.001	1.43	1.04–1.96	0.029
Entire set						
Age	1.02	1–1.04	0.041	1.03	1.01–1.05	0.001
Gender	1.11	0.73–1.69	0.616			
Tumour stage	2.21	1.73–2.81	< 0.001	2.52	1.93–3.28	< 0.001
Risk signature	1.92	1.59–2.32	< 0.001	1.94	1.6–2.36	< 0.001

Potential functions of PRlncRNAs and regulatory ceRNA network analysis

To further elucidate how PRlncRNAs regulate mRNA expression by sponging miRNAs in COAD, we identified 17 miRNAs (10 miRNAs for AP003555.1 and 7 miRNAs for LINC01133) that were predicted to be PRlncRNA targets after the four PRlncRNAs identified in our study were input into the LncBase v3 database, and 5706 mRNAs for these miRNAs were predicted via the ENCORI database (Additional Table 8). Then, Pearson correlation analysis between PRlncRNAs and mRNAs (Pearson's coefficient > 0.3 and $p < 0.001$) and between predictive miRNAs and selected mRNAs (Pearson's coefficient < − 0.3 and $P < 0.001$) was used to further identify regulatory ceRNA networks. Finally, Cytoscape was used to establish a ceRNA regulatory network (Fig. 10A). Moreover, according to the results of the GO functional enrichment analysis, all the target mRNAs were enriched in biological processes, such as regulation of cell population proliferation ($P =$ 1.81E- 06), regulation of hydrolase activity ($P =$ 4.83E-06), negative regulation of the extrinsic apoptotic signalling pathway ($P = 0.003$), regulation of the miRNA metabolic process ($P = 0.002$) and regulation of stem cell proliferation ($P = 0.002$) (Fig. 10B). These findings indicate that AP003555.1 may be involved in the regulation of tumour initiation and progression by acting as a ceRNA.

External dataset validation of the prognostic ability of the PRlncRNA risk signature

To further confirm the accuracy of the PRlncRNA risk signature in predicting patient prognosis, we used the Kaplan–Meier plotter database to examine the predictive significance of LINC01133 and FOXD3-AS1 in colon cancer, while AP001066.1 and AP003555.1 were not included in the database. Patients who exhibited elevated levels of LINC01133 experienced significantly shorter OS and RFS (HR > 1, $p < 0.05$; Fig. 11A, B) than those patients with reduced levels of this lncRNA. Patients with increased expression of FOXD3-AS1 exhibited a similar trend, while RFS was not significant (HR > 1 Fig. 11C, D). In summary, external database analysis provided clear validation of the ability of the PRlncRNA risk signature to evaluate the prognosis of patients with COAD.

Analysis of the expression level and biological function of AP003555.1

We confirmed the expression levels of AP003555.1 in eight paired samples from colon cancer patients at our institution.

Expression of AP003555.1 was elevated in tumour tissues compared with that in normal tissues (Fig. 12A). To further determine the function of AP003555.1 in colon cancer, we transfected LoVo and SW480 cells with si-AP003555.1 and negative control (NC). The results revealed that si-AP003555.1–1, − 2 and − 3 had

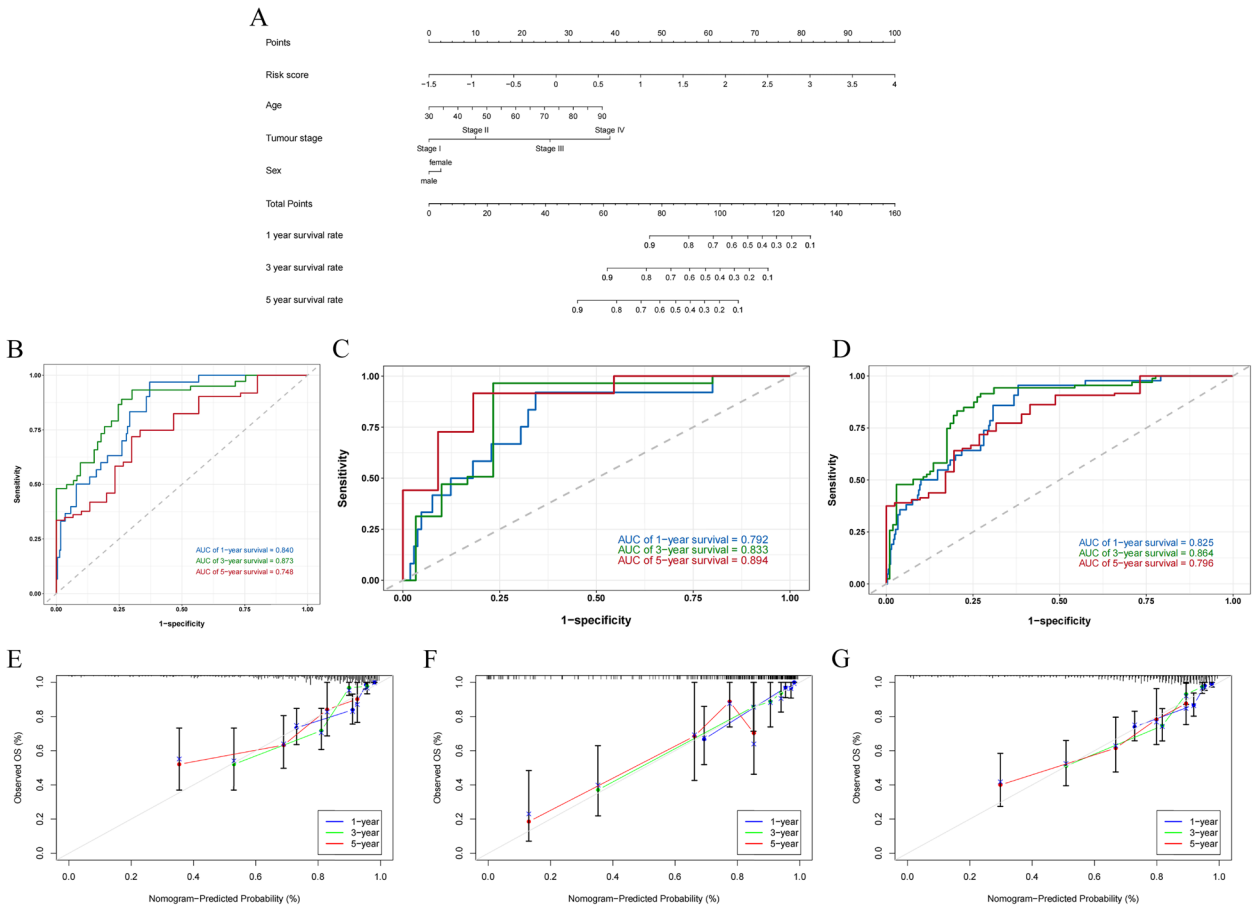

Fig. 6 Construction and evaluation of the nomogram for the risk score and clinicopathological characteristics. **A** A nomogram integrating the PRlncRNA risk score and clinicopathological characteristics for the prediction of 1-, 3-, and 5-year OS rates in the training set. The ROC analysis for assessing the predictive accuracy of the nomogram for 1-, 3-, and 5-year survival in the training set, (**B**), testing set (**C**), and entire set (**D**). Calibration curves of the nomogram for the probability of OS at 1, 3, and 5 years in the training set (**E**), testing set (**F**), and entire set (**G**)

high knockdown efficiencies (Fig. 12B). We found that AP003555.1 knockdown inhibited the viability (Fig. 12C) and proliferation (Fig. 12D) of colon cancer cells. The results of flow cytometry revealed a significant increase in the percentage of apoptotic cells in the si-AP003555.1 group compared with that in the NC group (Fig. 13A, B).

Discussion

Recent studies have shown that extensive cross-talk occurs in cells under pathological conditions, making PCD a mixed form of biological process. PANoptosis, which is regulated by the PANoptosome complex, is a unique form of PCD that involves pyroptosis, apoptosis and necroptosis. This multifaceted process has garnered significant interest among researchers in recent years [34]. Malireddi et al. demonstrated that the combination of TNF-α and IFN-γ plays a crucial role in promoting tumour cell death through the JAK-STAT1-IRF1 pathway, which acts as an effective inducer of PANoptosis [35]. In addition, another study revealed that sulfaconazole could increase the radiosensitivity of oesophageal cancer cells by inducing oxidative stress and PANoptosis [36]. Indeed, lncRNAs have emerged as crucial players in PCD, impacting various processes, including apoptosis, pyroptosis, necrosis and autophagy [37, 38]. Notably, two studies successfully developed prognostic risk models for identifying high-risk patients and refining the risk prognosis in patients with thyroid cancer and renal clear cell carcinoma. These models are based on seven and five PRlncRNAs, respectively [27, 39]. However, confirmed PRlncRNAs and identification of high-risk patients with COAD are still lacking. Therefore, a pressing need exists to widely identify PRlncRNAs and establish a prognostic risk model to guide the management of and individualized therapeutic methods for patients with COAD.

In our study, we established a risk signature comprising four PRlncRNAs capable of effectively stratifying patients into high- and low-risk groups. The ROC curve

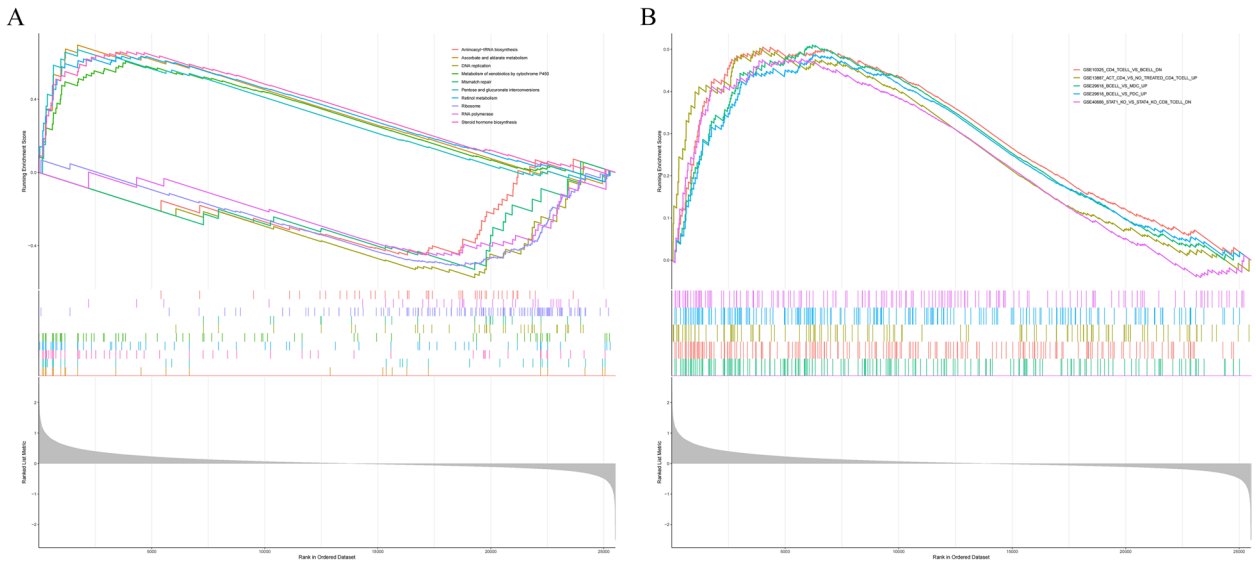

Fig. 7 Functional GSEA of the PRlncRNA risk signature. **A** Significantly enriched GSEA pathways in the high- and low-risk groups. **B** Immune-related processes significantly enriched in the high-risk group

analysis with corresponding AUC values demonstrated the moderate predictive performance of the PRlncRNA risk signature across the three sets. Furthermore, univariate and multivariate Cox regression analyses highlighted the independent prognostic value of the prognostic risk model in predicting OS among patients with COAD. Additionally, the development of a novel nomogram provided a visually intuitive tool for predicting the 1-, 3-, and 5-year survival rates of individual patients with COAD, thus facilitating improved clinical decision making.

The lncRNAs LINC01133, FOXD3-AS1, AP001066.1 and AP003555.1 were identified in our study. The high expression of the four identified PRlncRNAs in the high-risk group suggested their potential association with poor prognosis among patients with COAD. One study reported that LINC01133 functions as both a cancer suppressor and a ceRNA in digestive system tumours [40]. Zhang et al. reported significant downregulation of LINC01133 in CRC tissues compared with that in normal tissue samples. Moreover, they observed that a low expression level of LINC01133 was significantly associated with metastasis [41]. A study suggested that propofol-induced LINC01133 weakened the proliferation, migration and invasion of CRC cell lines through the miR- 186 - 5p/NR3 C2 axis [42]. However, Lin et al. demonstrated that LINC01133 promoted hepatocellular carcinoma progression by sponging miR-199a-5p and interacting with the Annexin A2/STAT3 signalling pathway [43]. Wu et al. demonstrated that the inhibition of FOXD3-AS1 suppressed CRC progression and promoted cell apoptosis through the miR- 135a- 5p/SIRT1 axis [44]. Moreover, we demonstrated that the expression level of AP001066.1 was positively correlated with that of TLR9. However, there are currently no studies associated with AP001066.1, indicating the need for further research in this area. The lncRNA AP003555.1 has been demonstrated in previous studies to be closely related to colon cancer prognosis, with high expression observed in tumour tissue, which is consistent with our findings [13, 45, 46]. However, the mechanism of AP003555.1 in COAD has not previously been reported in the literature. Our study revealed that AP003555.1 is associated with prognosis in patients with COAD and that the expression level of AP003555.1 was significantly correlated with that of CASP4. In addition, we constructed a ceRNA regulatory network associated with AP003555.1 and predicted that AP003555.1 may be involved in the regulation of tumour initiation and progression by acting as an endogenous competing RNA of hsa-miR- 17 - 5p and hsa-miR-93 - 5p. Functionally, different experiments revealed that AP003555.1 promoted the proliferation and viability and inhibited the apoptosis of colon cancer cells.

The potential pathways related to the PRlncRNA risk signature were investigated through GSEA, which revealed that metabolic pathways were enriched in the high-risk group. Studies have shown that LINC01133 participates in various metabolic processes. Ding et al. reported that LINC01133 is upregulated and interacts with miR- 3065 to increase ADH7 expression, promoting metabolism in cervical cancer [47]. Additionally, Foroughi et al. reported that LINC01133 is downregulated in gastric cancer and is involved mainly in metabolic

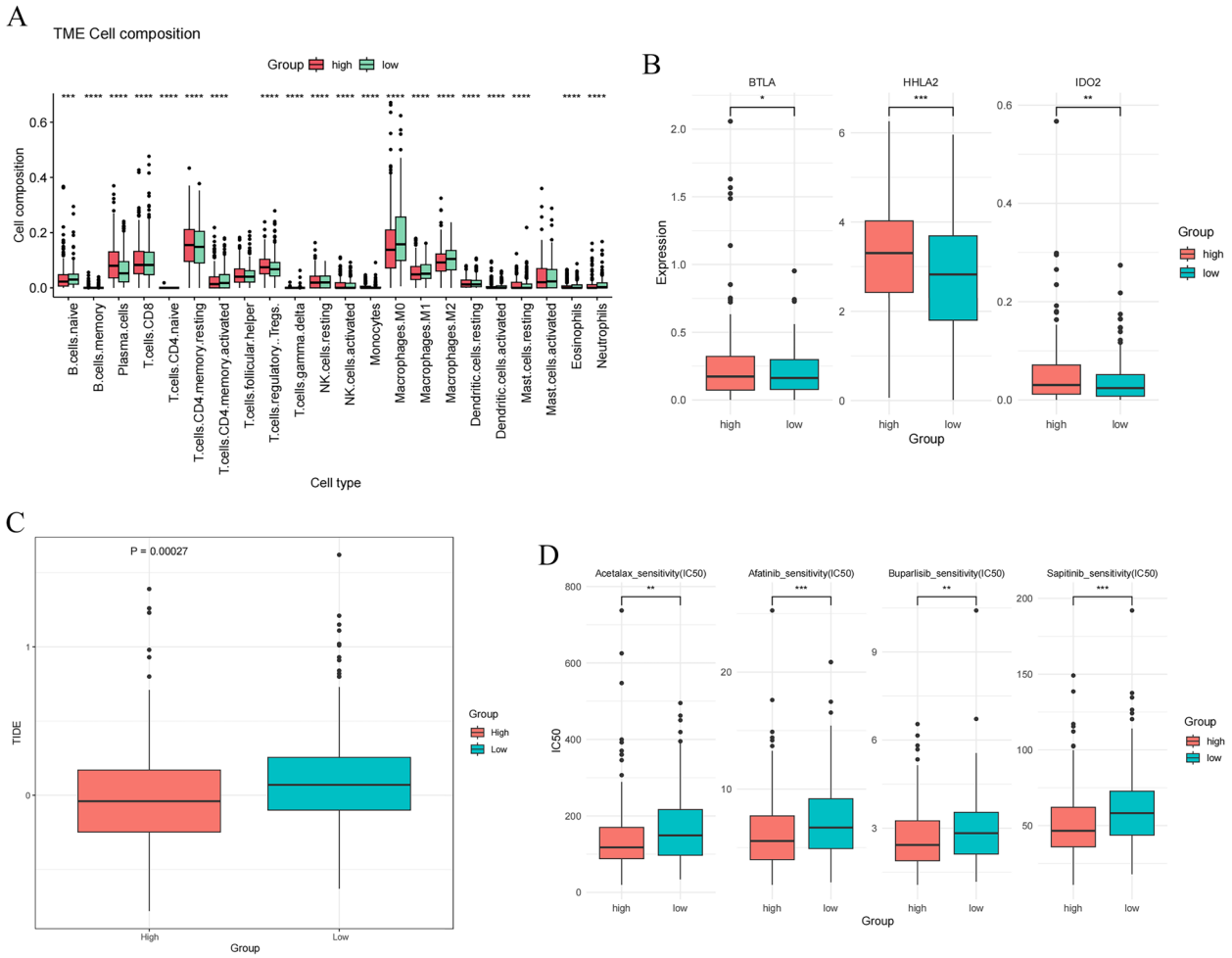

Fig. 8 Analysis of immune infiltration and prediction of response to immunotherapy and antitumour drugs. **A** Boxplots of all immune responses across the two groups based on the CIBERSORT algorithm. **B** Expression levels of three immune checkpoint genes in the two groups. **C** Comparison of TIDE prediction scores across the two groups. **D** Assessment of sensitivity to antitumour drugs (doxorubicin, gemcitabine, bleomycin, and paclitaxel) in the two groups

pathways and networks related to gastrointestinal diseases and functions [48]. However, further experiments are needed to verify the roles of PRlncRNAs in metabolism.

Moreover, we confirmed that a high PRlncRNA risk score was associated with numerous immune processes. Tumour cells promote tumour progression by relying on immune suppression in the host to evade immune surveillance. Regulatory T cells, which are common immunosuppressive cells in the tumour microenvironment, inhibit antitumour immune responses through various mechanisms in COAD [49, 50]. Our results indicated that regulatory T cells were enriched in the high-risk group. Tumour immune escape is associated with a decrease in T-cell responses, which are manifested mainly by the inhibition of $CD8^+$ T-cell activation and immune tolerance to $CD4^+$ T cells [51]. Notably, the high-risk group presented elevated levels of activated $CD8^+$ T cells, potentially due to the presence of numerous immunosuppressive factors within the tumour microenvironment, which significantly inhibited the antitumour activity of $CD8^+$ T cells [52]. Tumour-associated macrophages (TAMs) play crucial roles in various aspects of colon cancer, including tumour angiogenesis and metastasis. Two main phenotypes of TAMS, M1 and M2, often exhibit contrasting effects on tumour progression (M1: antitumour function; M2: protumour function) [53]. However, we found that M1 and M2 were both expressed at low levels in high-risk populations. This may be significantly correlated with the rapid vascular growth and macrophage infiltration of tumour cells under hypoxic conditions [54]. The reason may be that the patients with COAD in our study were mainly in the early stage (57%), which is a low-hypoxic condition, resulting in slow

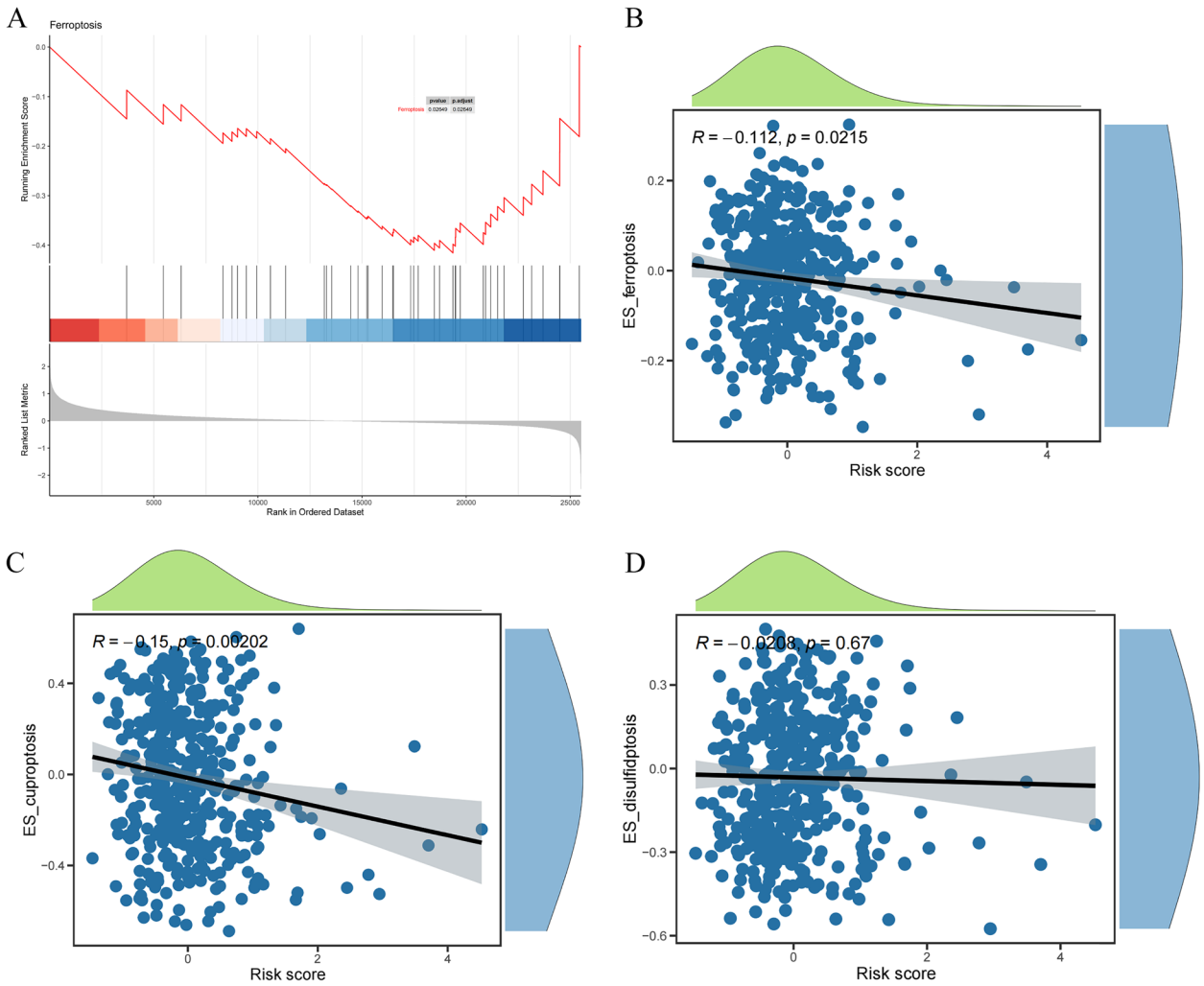

Fig. 9 Association between ferroptosis, cuproptosis, disulfidptosis and the PRlncRNA risk signature. **A** Ferroptosis was enriched in the low-risk group. **B** The ES of ferroptosis was negatively correlated with the risk score. **C** The ES for cuproptosis was negatively correlated with the risk score. **D** The ES of disulfidptosis patients did not significantly differ from the risk score

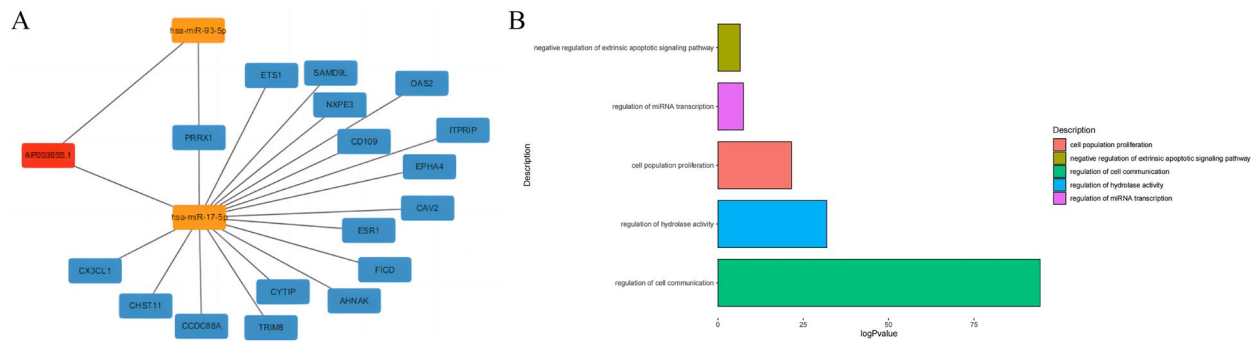

Fig. 10 ceRNA network and potential functions of PRlncRNAs. **A** A ceRNA network constructed with AP003555.1. **B** The five results of the Gene Ontology functional enrichment analysis

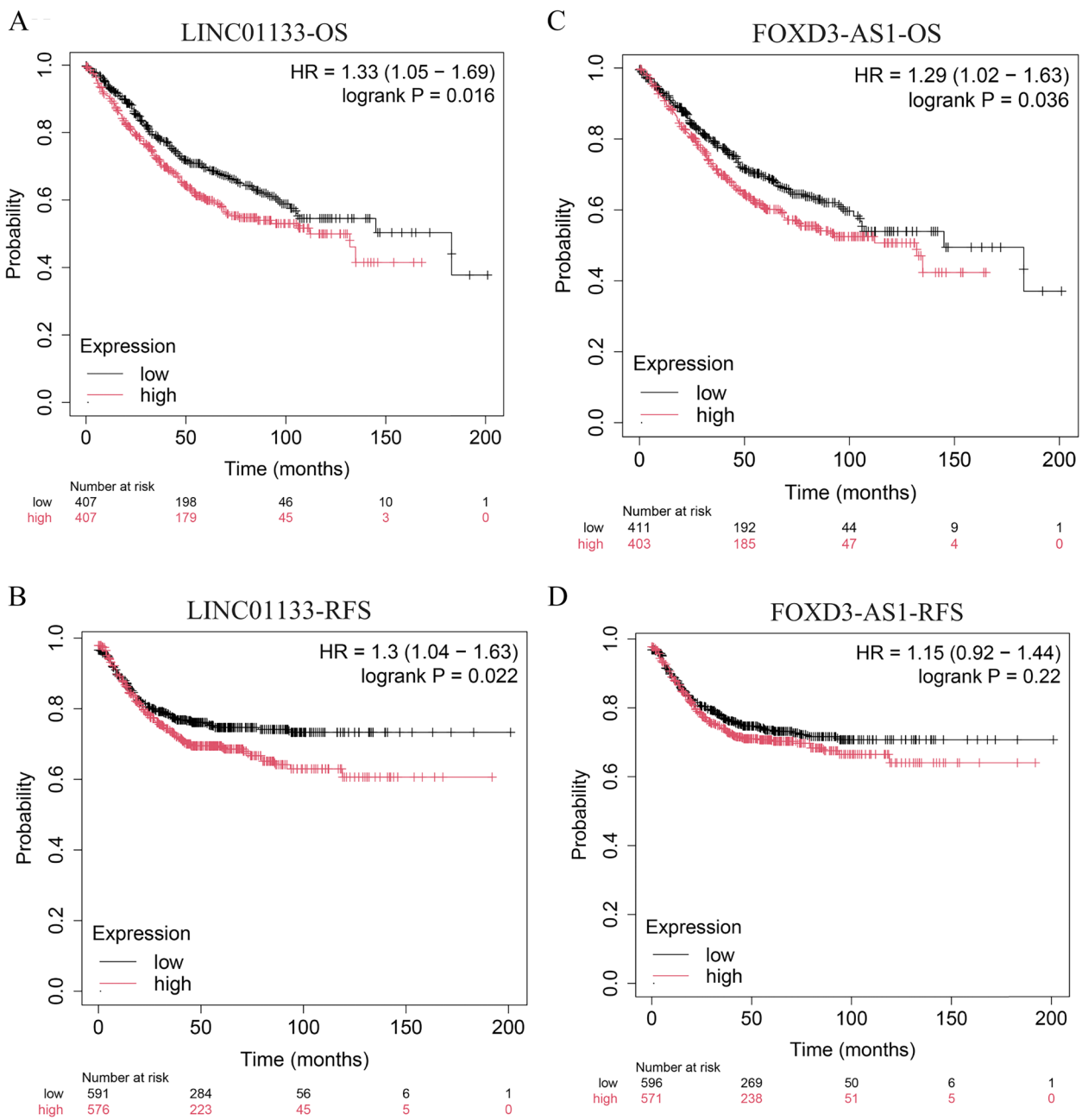

Fig. 11 Validation of PRlncRNAs as possible biomarkers in the external dataset. Overall survival (OS) and recurrence-free survival (RFS) analysis of LINC01133 (**A**, **B**) and FOXD3-AS1 (**C**, **D**) from the Kaplan–Meier plotter database

tumour cell growth [55]. These findings suggest that the poorer prognosis observed in high-risk patients could be attributed to reduced immunoreactivity within the tumour microenvironment.

Patients with various malignant tumours can benefit from immune checkpoint inhibitor therapy [56]. Zhang et al. reported that the blood expression levels of TIM- 3, LAG- 3, CTLA- 4 and BTLA were significantly increased and strongly associated with survival in CRC patients [57]. Kamal et al. demonstrated that CD160, TNFSF15, HHLA2, IDO2 and KIR3DL1 were highly relevant to the tumour immune microenvironment of CRC [58]. As in prior studies, the PRlncRNA risk score was positively correlated with the expression levels of immune checkpoint genes (BTLA, HHLA2, and IDO2). Additionally, patients with COAD in the high-risk group

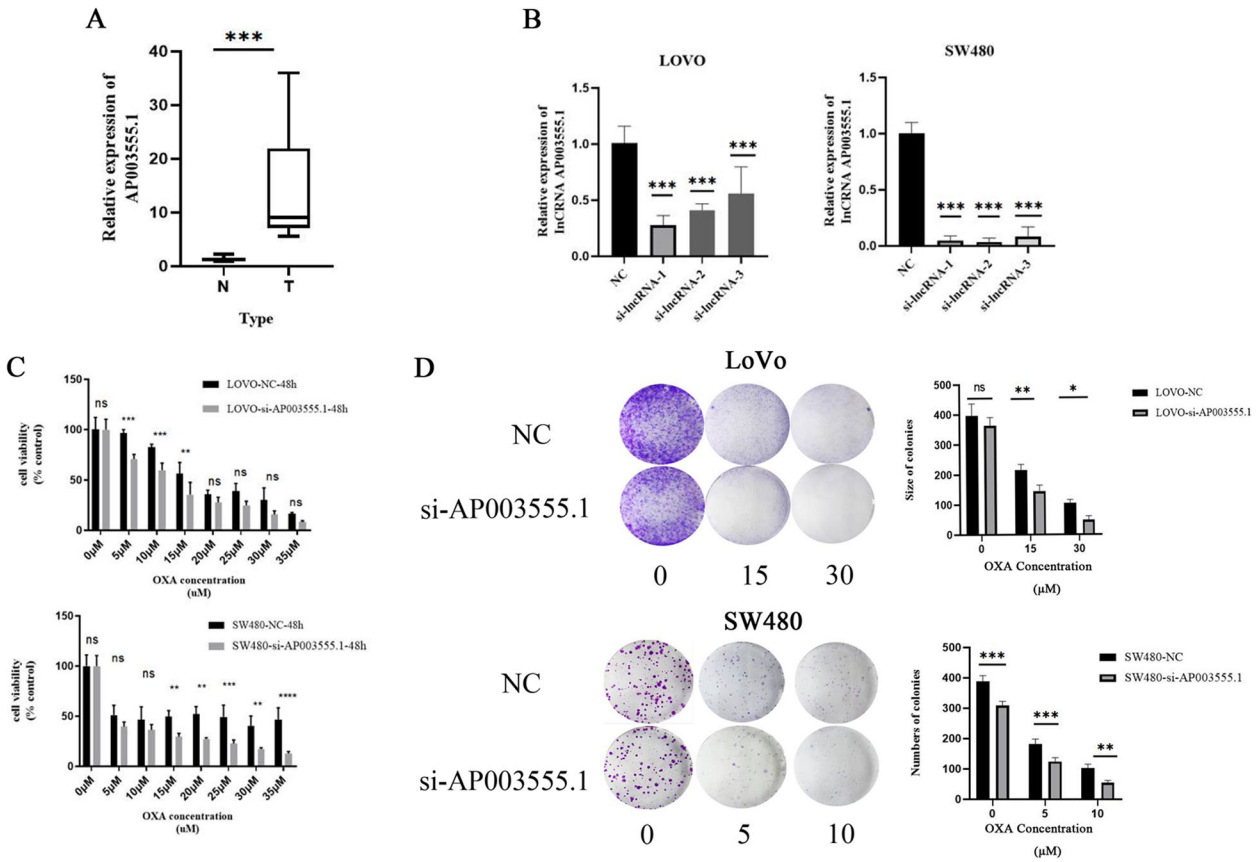

Fig. 12 Validation of the expression level and biological function of AP003555.1. **A** The expression level of AP003555.1 in eight pairs of colon cancer tissue samples. **B** QPCR analysis of AP003555.1 expression levels in colon cancer cells transfected with specific siRNAs as indicated. **C** Cell viability after AP003555.1 knockdown. **D** Cell proliferation capacity after AP003555.1 knockdown

presented notably lower TIDE scores, suggesting a potentially improved response to immunotherapy. Gao et al. reported that sapitinib significantly enhanced the effectiveness of paclitaxel and doxorubicin in ABCB1-overexpressing colon cells, suggesting a reversal of anticancer drug resistance [59]. Razali et al. reported that buparlisib treatment significantly decreased apoptosis in ulcerative colitis and CRC cells by preventing PI3 K activation [60]. Afatinib exhibited inhibitory effects on CRC cells overexpressing HER2 both in vitro and in vivo [61]. Similarly, the IC50 values of sapitinib, buparlisib, and afatinib were lower in the high-risk group than in the low-risk group.

Ferroptosis, cuproptosis and disulfidptosis are three newly identified types of PCD and are associated with lncRNAs in colon cancer. Notably, the GSEA and GSVA results indicated that the"ferroptosis"pathway was enriched in the low-risk group and that ferroptosis and cuproptosis were negatively correlated with PRlncRNA risk scores. Previous studies have revealed that ferroptosis and cuproptosis have inhibitory effects on the development of CRC [62–65], which may help explain the better prognosis in the low-risk group of patients with COAD in this study. Moreover, previous studies have shown that AP003555.1 is linked to ferroptosis and is correlated with prognosis in CRC [66] and COAD [67]. In addition, another study demonstrated that AP003555.1 is a disulfidptosis-related lncRNA [13, 46]. In contrast, the GSVA results revealed that the PRlncRNA risk score was not significantly associated with disulfidptosis, which may be influenced by three other lncRNAs. These results also indirectly suggest that ferroptosis and cuproptosis may be related to PANoptosis.

First, we developed a new prognostic model based on PRlncRNAs to reliably predict the prognosis of patients with COAD, which is beneficial for developing personalized treatments for patients with COAD, including immunotherapy and chemotherapy. Second, we demonstrated that four PRlncRNAs, particularly AP003555.1, have the potential to become new therapeutic targets and biomarkers for COAD and are associated with PANoptosis. Third, we speculate that PANoptosis is

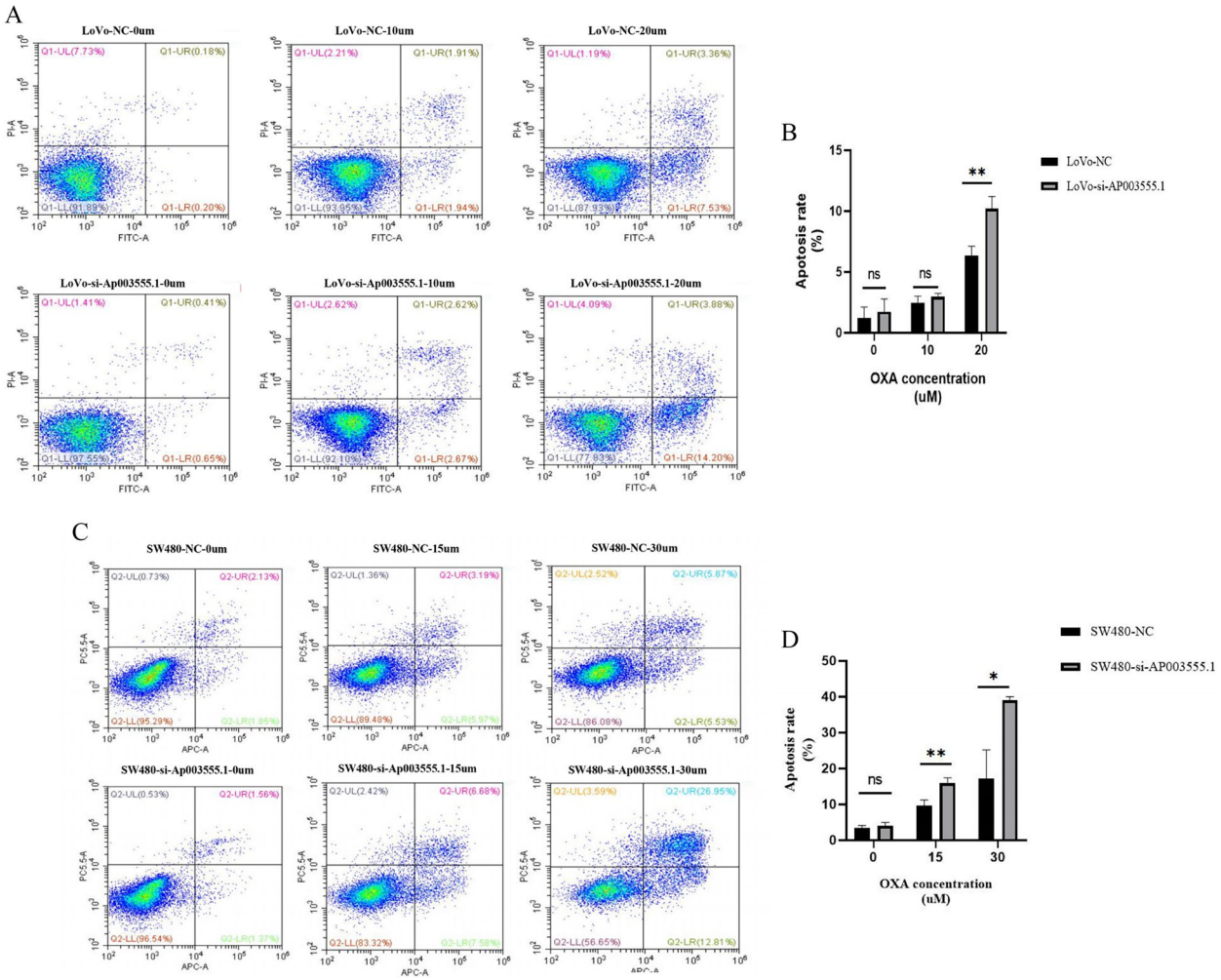

Fig. 13 The percentage of apoptotic colon cancer cells in the si-AP003555.1 and NC groups treated with different oxaliplatin concentrations**.** The rates of apoptosis induction in LoVo (**A**) and SW480 (**B**) cells in the two groups were evaluated via V-FITC/PI staining

closely related to cuproptosis and ferroptosis, but more research is needed to prove this hypothesis.

The current study had several limitations. First, PANoptosis is a newly discovered form of PCD, and research and databases on this topic are limited. Therefore, we included only 32 PRGs based on a limited number of research results, which may affect the comprehensiveness of the results presented in this article. In future research, we will comprehensively summarize and analyse all published literature and related databases to provide a more comprehensive and accurate analysis. Second, owing to the limited research on the four selected PRlncRNAs, we were unable to obtain comprehensive lncRNA annotations and clinical information from databases such as the Gene Expression Omnibus. This limitation highlights the sustained importance of lncRNAs, and the limitations of current technology still partially mask the importance of lncRNAs. Although two PRlncRNAs have been confirmed through an external Kaplan–Meier mapping database (GEO), further validation of risk characteristics requires an independent colon cancer cohort to enhance its credibility and robustness. Third, although we conducted qPCR to examine the expression levels of AP003555.1 in eight paired clinical samples, the limited sample size used in our study was a limiting factor. Conducting larger-scale studies with sufficient sample sizes will provide stronger evidence and validate the prognostic significance of the model. Finally, the mechanisms by which these PRlncRNAs affect the immune landscape and drug sensitivity are still unknown. Additional extensive research is needed to examine the complex associations between these lncRNAs and DRGs, with the aim of revealing potential targets for successful treatment methods.

Conclusions

In conclusion, we established a PRlncRNA risk signature comprising four lncRNAs (LINC01133, FOXD3-AS1, AP001066.1, and AP003555.1) in COAD and revealed that AP003555.1 facilitates the viability and proliferation and suppresses the apoptosis of colon cancer cells.

Abbreviations

PCD	Programmed cell death
LncRNA	Long non-coding RNA
PRLncRNA	PANoptosis-related lncRNA
COAD	Colon adenocarcinoma
TCGA	The Cancer Genome Atlas
ceRNA	Competing endogenous RNA
GO	Gene ontology
siRNA	Small interfering RNA
qPCR	Quantitative Polymerase Chain Reaction
CRC	Colorectal cancer
FPKM	Fragments per kilobase of transcript per million reads mapped
OS	Overall survival
PRGs	PANoptosis-related genes
KEGG	Kyoto Encyclopedia of Genes and Genomes
LASSO	Least absolute shrinkage and selection operator
K-M	Kaplan–Meier
ROC	Receiver operating characteristic
AUC	Area under the curve
GSEA	Gene set enrichment analysis
TIDE	Tumor Immune Dysfunction and Exclusion
IC50	Half inhibitory concentration
ES	Enrichment score
GSVA	Gene set variation analysis
miRNAs	MicroRNAs
ENCORI	Encyclopaedia of RNA Interactomes
RFS	Recurrence free survival
CCK- 8	Cell counting kit- 8
NC	Negative control
PBS	Phosphate buffered solution
PI	Propidium iodide
TAMs	Tumor-associated macrophages

Supplementary Information

The online version contains supplementary material available at https://doi.org/10.1186/s12885-025-14021-2.

Additional file 1. Table 1. Survival information and clinical characteristics of 468 eligible patients with COAD. The patient ID, survival status, survival time, sex, age and tumour stage are listed. Table 2. Clinical characteristics of eight patients. The patients' ID, sex, age and tumour stage are listed. Table 3. The sequences of AP003555.1 and actin. The sequences of the primers used for amplifying AP003555.1 and actin are listed. Table 4. The gene set of 32 PANoptosis-related genes. Thirty-two PANoptosis-related genes are presented. Table 5. A total of 1086 PANoptosis-related differentially expressed lncRNAs. The Pearson correlation coefficient (cor_R) and p value (cor_P) based on Pearson correlation analysis are listed. Table 6. Univariate Cox regression analysis of the PANoptosis-related lncRNAs. The hazard ratios, 95% confidence intervals and p values are listed, and statistically significant PANoptosis-related lncRNAs are labelled as significant. Table 7. The gene sets of 19 genes related to cuproptosis and 26 related to disulfidptosis were obtained from previous literature. Nineteen genes related to cuproptosis and 26 related to disulfidptosis are presented. Table 8. Summary of the prediction of miRNAs and mRNAs of PANoptosis-related lncRNAs. Seventeen miRNAs (10 miRNAs for AP003555.1 and seven miRNAs for LINC01133) were identified from the LncBase v3 database, and 5706 mRNAs for the miRNAs were identified from the ENCORI database. Figure 1. Volcano plot of the differentially expressed lncRNAs between normal and tumour samples. A total of 2159 differentially expressed lncRNAs between normal and tumour samples were identified. The red genes are upregulated genes, the grey genes are unchanged genes, and the blue genes are downregulated.

Acknowledgements

The authors express gratitude to Weixin Wang, Xiaojun Peng and Cifeng Cai from Hangzhou Cosmos Wisdom for their technical support in data analysis.

Authors' contributions

Yuekai Cui, Jie Mei and Shengsheng Zhao conceived and designed the experiments, performed the experiments. Bingzi Zhu and Binglong Bai analyzed the data. Shangrui Rao,Weijian Sun and Jianhua Lu performed the experiments, prepared manuscript. Hongzheng Li and Wenyu Jin prepared figures and tables. Yongdong Yi, Xueqiong Zhu ,Shangrui Rao and Weijian Sun authored and reviewed drafts of the article, and approved the final draft.

Funding

This work was supported by the Clinical Research Foundation of The Second Affiliated Hospital of Wenzhou Medical University (Project No. SAHoWMU-CR2019-02-214), the National Natural Science Foundation of China (Grant Number 81972261，82272172), the Major Research Projects of Wenzhou Science and Technology Plan Project(Grant Numbers ZY2020007, Y20210189, ZY2021003 and Y2020154), the Key Project Cultivation Project of Wenzhou Medical University (Grant Number KYYW202006), Medical Health Science and Technology key Project of Zhejiang Provincial and Ministry Health Commission（WKJ-ZJ-2322）, Lin He's New Medicine and Clinical Translation Academician Workstation Research Fund(Grant Numbers 18331202 and 19331104), the Natural Science Foundation of Zhejiang Province (Grant Number LY18H030009) and the Project of Medical Technology and Education of Zhejiang Province of China (Grant Number 202045547).

Data availability

The datasets analyzed for this study can be found in the TCGA (TCGA-COAD, https://portal.gdc.cancer.gov).

Declarations

Ethics approval and consent to participate

The study was performed in accordance with the Declaration of Helsinki. The following information was supplied relating to ethical approvals: The 2nd Affiliated Hospital and Yuying Children's Hospital of Wenzhou Medical University granted Ethical approval to carry out the study within its facilities (Ethical Application Ref: 2023-K- 247–02). The need for informed consent was waived by Article 32 of China's Measures for the Ethical Review of Life Science and Medical Research Involving Humans, which permits exemption from individual consent for low-risk studies utilizing non-sensitive, anonymized data. Given that the data from the TCGA and Kaplan–Meier plotter databases are publicly available, we did not require informed patient consent in this retrospective population-based cohort study.

Consent for publication

Not applicable.

Competing interests

The authors declare no competing interests.

Author details

[1]Second Affiliated Hospital & Yuying Childrens' & Hospital of Wenzhou Medical University, Wenzhou, China. [2]First Affiliated Hospital of Wenzhou Medical University, Wenzhou, China. [3]Wenzhou Medical University, Wenzhou, China.

Received: 6 June 2024 Accepted: 26 March 2025
Published online: 10 April 2025

References

1. Siegel RL, Miller KD, Wagle NS, Jemal A. Cancer statistics, 2023. CA Cancer J Clin. 2023;73(1):17–48.
2. Hossain MS, Karuniawati H, Jairoun AA, Urbi Z, Ooi J, John A, et al. Colorectal cancer: a review of carcinogenesis, global epidemiology, current challenges, risk factors, preventive and treatment strategies. Cancers (Basel). 2022;14(7):1732.
3. Ahmed M. Colon Cancer: A Clinician's Perspective in 2019. Gastroenterology Res. 2020;13(1):1–10.
4. Jiang HH, Xing SW, Tang X, Chen Y, Lin K, He LW, et al. Novel multiplex stool-based assay for the detection of early-stage colon cancer in a Chinese population. World J Gastroenterol. 2022;28(24):2705–32.
5. Alrushaid N, Khan FA, Al-Suhaimi E, Elaissari A. Progress and perspectives in colon cancer pathology, diagnosis, and treatments. Diseases. 2023;11(4):148.
6. Meropol NJ, Berger NA. Colon cancer recurrence: insights from the interface between epidemiology, laboratory science, and clinical medicine. J Natl Cancer Inst. 2012;104(22):1697–8.
7. Iyer MK, Niknafs YS, Malik R, Singhal U, Sahu A, Hosono Y, et al. The landscape of long noncoding RNAs in the human transcriptome. Nat Genet. 2015;47(3):199–208.
8. Chen S, Shen X. Long noncoding RNAs: functions and mechanisms in colon cancer. Mol Cancer. 2020;19(1):167.
9. Tang X, Qiao X, Chen C, Liu Y, Zhu J, Liu J. Regulation Mechanism of Long Noncoding RNAs in Colon Cancer Development and Progression. Yonsei Med J. 2019;60(4):319–25.
10. Lin Y, Li Y, Chen Y, Zhang Z. LncRNA ALMS1-IT1 is a novel prognostic biomarker and correlated with immune infiltrates in colon adenocarcinoma. Medicine (Baltimore). 2022;101(42): e31314.
11. Cen X, Huang Y, Lu Z, Shao W, Zhuo C, Bao C, et al. LncRNA IGFL2-AS1 Promotes the Proliferation, Migration, and Invasion of Colon Cancer Cells and is Associated with Patient Prognosis. Cancer Manag Res. 2021;13:5957–68.
12. Li X, Lei J, Shi Y, Peng Z, Gong M, Shu X. Developing a RiskScore Model based on Angiogenesis-related lncRNAs for Colon Adenocarcinoma Prognostic Prediction. Curr Med Chem. 2024;31(17):2449–66.
13. Dong X, Liao P, Liu X, Yang Z, Wang Y, Zhong W, et al. Construction and validation of a reliable disulfidptosis-related LncRNAs signature of the subtype, prognostic, and immune landscape in colon cancer. Int J Mol Sci. 2023;24(16):12915.
14. Salmena L, Poliseno L, Tay Y, Kats L, Pandolfi PP. A ceRNA hypothesis: the Rosetta Stone of a hidden RNA language? Cell. 2011;146(3):353–8.
15. Cheng Y, Geng L, Wang K, Sun J, Xu W, Gong S, Zhu Y. Long Noncoding RNA Expression Signatures of Colon Cancer Based on the ceRNA Network and Their Prognostic Value. Dis Markers. 2019;2019:7636757.
16. Li KZ, Yin YX, Tang YP, Long L, Xie MZ, Li JL, et al. Construction of a long noncoding RNA-based competing endogenous RNA network and prognostic signatures of left- and right-side colon cancer. Cancer Cell Int. 2021;21(1):211.
17. Fang C, Qiu S, Sun F, Li W, Wang Z, Yue B, et al. Long non-coding RNA HNF1A-AS1 mediated repression of miR-34a/SIRT1/p53 feedback loop promotes the metastatic progression of colon cancer by functioning as a competing endogenous RNA. Cancer Lett. 2017;410:50–62.
18. Wang L, Wei Z, Wu K, Dai W, Zhang C, Peng J, He Y. Long noncoding RNA B3GALT5-AS1 suppresses colon cancer liver metastasis via repressing microRNA-203. Aging (Albany NY). 2018;10(12):3662–82.
19. Jing X, Du L, Shi S, Niu A, Wu J, Wang Y, Wang C. Hypoxia-Induced Upregulation of lncRNA ELFN1-AS1 Promotes Colon Cancer Growth and Metastasis Through Targeting TRIM14 via Sponging miR-191-5p. Front Pharmacol. 2022;13: 806682.
20. Wong RS. Apoptosis in cancer: from pathogenesis to treatment. J Exp Clin Cancer Res. 2011;30(1):87.
21. Wei X, Xie F, Zhou X, Wu Y, Yan H, Liu T, et al. Role of pyroptosis in inflammation and cancer. Cell Mol Immunol. 2022;19(9):971–92.
22. Gong Y, Fan Z, Luo G, Yang C, Huang Q, Fan K, et al. The role of necroptosis in cancer biology and therapy. Mol Cancer. 2019;18(1):100.
23. Malireddi RKS, Kesavardhana S, Kanneganti TD. ZBP1 and TAK1: Master Regulators of NLRP3 Inflammasome/Pyroptosis, Apoptosis, and Necroptosis (PAN-optosis). Front Cell Infect Microbiol. 2019;9:406.
24. Wang X, Sun R, Chan S, Meng L, Xu Y, Zuo X, et al. PANoptosis-based molecular clustering and prognostic signature predicts patient survival and immune landscape in colon cancer. Front Genet. 2022;13: 955355.
25. Huang J, Jiang S, Liang L, He H, Liu Y, Cong L, Jiang Y. Analysis of PANoptosis-Related LncRNA-miRNA-mRNA Network Reveals LncRNA SNHG7 Involved in Chemo-Resistance in Colon Adenocarcinoma. Front Oncol. 2022;12: 888105.
26. Wei Y, Lan C, Yang C, Liao X, Zhou X, Huang X, et al. Robust analysis of a novel PANoptosis-related prognostic gene signature model for hepatocellular carcinoma immune infiltration and therapeutic response. Sci Rep. 2023;13(1):14519.
27. Li R, Zhao M, Sun M, Miao C, Lu J. Construction and validation of a PANoptosis-related lncRNA signature for predicting prognosis and targeted drug response in thyroid cancer. PeerJ. 2023;11: e15884.
28. Li J, Wu F, Li C, Sun S, Feng C, Wu H, et al. The cuproptosis-related signature predicts prognosis and indicates immune microenvironment in breast cancer. Front Genet. 2022;13: 977322.
29. Wang F, Lin H, Su Q, Li C. Cuproptosis-related lncRNA predict prognosis and immune response of lung adenocarcinoma. World J Surg Oncol. 2022;20(1):275.
30. Chen X, Wang Z, Wu Y, Lan Y, Li Y. Typing and modeling of hepatocellular carcinoma based on disulfidptosis-related amino acid metabolism genes for predicting prognosis and guiding individualized treatment. Front Oncol. 2023;13:1204335.
31. Li Q, Yin LK. Comprehensive analysis of disulfidptosis related genes and prognosis of gastric cancer. World J Clin Oncol. 2023;14(10):373–99.
32. Liu S, Zheng Y, Li S, Du Y, Liu X, Tang H, et al. Integrative landscape analysis of prognostic model biomarkers and immunogenomics of disulfidptosis-related genes in breast cancer based on LASSO and WGCNA analyses. J Cancer Res Clin Oncol. 2023;149(18):16851–67.
33. Li J, Yang C, Zheng Y. A novel disulfidptosis and glycolysis related risk score signature for prediction of prognosis and ICI therapeutic responsiveness in colorectal cancer. Sci Rep. 2023;13(1):13344.
34. Liu J, Hong M, Li Y, Chen D, Wu Y, Hu Y. Programmed Cell Death Tunes Tumor Immunity. Front Immunol. 2022;13: 847345.
35. Malireddi RKS, Karki R, Sundaram B, Kancharana B, Lee S, Samir P, Kanneganti TD. Inflammatory Cell Death, PANoptosis, Mediated by Cytokines in Diverse Cancer Lineages Inhibits Tumor Growth. Immunohorizons. 2021;5(7):568–80.
36. Liu LX, Heng JH, Deng DX, Zhao H, Zheng ZY, Liao LD, et al. Sulconazole Induces PANoptosis by Triggering Oxidative Stress and Inhibiting Glycolysis to Increase Radiosensitivity in Esophageal Cancer. Mol Cell Proteomics. 2023;22(6): 100551.
37. Gao L, Jiang Z, Han Y, Li Y, Yang X. Regulation of Pyroptosis by ncRNA: A Novel Research Direction. Front Cell Dev Biol. 2022;10: 840576.
38. Jiang N, Zhang X, Gu X, Li X, Shang L. Progress in understanding the role of lncRNA in programmed cell death. Cell Death Discov. 2021;7(1):30.
39. Liu W, Qu C, Wang X. Comprehensive analysis of the role of immune-related PANoptosis lncRNA model in renal clear cell carcinoma based on RNA transcriptome and single-cell sequencing. Oncol Res. 2023;31(4):543–67.
40. Jiang S, Zhang Q, Li J, Raziq K, Kang X, Liang S, et al. New Sights Into Long Non-Coding RNA LINC01133 in Cancer. Front Oncol. 2022;12: 908162.
41. Zhang JH, Li AY, Wei N. Downregulation of long non-coding RNA LINC01133 is predictive of poor prognosis in colorectal cancer patients. Eur Rev Med Pharmacol Sci. 2017;21(9):2103–7.
42. Yao Y, Zhang F, Liu F, Xia D. Propofol-induced LINC01133 inhibits the progression of colorectal cancer via miR-186-5p/NR3C2 axis. Environ Toxicol. 2024;39(4):2265–84.
43. Yin D, Hu ZQ, Luo CB, Wang XY, Xin HY, Sun RQ, et al. LINC01133 promotes hepatocellular carcinoma progression by sponging miR-199a-5p and activating annexin A2. Clin Transl Med. 2021;11(5): e409.
44. Wu Q, Shi M, Meng W, Wang Y, Hui P, Ma J. Long noncoding RNA FOXD3-AS1 promotes colon adenocarcinoma progression and functions as a competing endogenous RNA to regulate SIRT1 by sponging miR-135a-5p. J Cell Physiol. 2019;234(12):21889–902.
45. Wu Z, Lu Z, Li L, Ma M, Long F, Wu R, et al. Identification and Validation of Ferroptosis-Related LncRNA Signatures as a Novel Prognostic Model for Colon Cancer. Front Immunol. 2021;12: 783362.
46. Chen P, Yu J, Luo Q, Li J, Wang W. Construction of disulfidptosis-related lncRNA signature for predicting the prognosis and immune escape in colon adenocarcinoma. BMC Gastroenterol. 2023;23(1):382.

47. Ding S, Huang X, Zhu J, Xu B, Xu L, Gu D, Zhang W. ADH7, miR-3065 and LINC01133 are associated with cervical cancer progression in different age groups. Oncol Lett. 2020;19(3):2326–38.
48. Foroughi K, Amini M, Atashi A, Mahmoodzadeh H, Hamann U, Manoochehri M. Tissue-specific down-regulation of the long non-coding RNAs PCAT18 and LINC01133 in gastric cancer development. Int J Mol Sci. 2018;19(12):3881.
49. Taheri RA, Bahramifar A, Jaafari MR, Fasihi-Ramandi M, Emameh RZ, Mohammadian Haftcheshmeh S, Ebrahimi NM. Designing new nanoliposomal formulations and evaluating their effects on myeloid-derived suppressor cells and regulatory T cells in a colon cancer model aiming to develop an efficient delivery system for cancer treatment; an in vitro and in vivo study. Biotechnol Appl Biochem. 2022;69(5):2151–60.
50. Erdman SE, Poutahidis T. Roles for inflammation and regulatory T cells in colon cancer. Toxicol Pathol. 2010;38(1):76–87.
51. Yang X, Wu W, Pan Y, Zhou Q, Xu J, Han S. Immune-related genes in tumor-specific CD4(+) and CD8(+) T cells in colon cancer. BMC Cancer. 2020;20(1):585.
52. Liu C, Liu D, Wang F, Liu Y, Xie J, Xie J, Xie Y. Construction of a novel choline metabolism-related signature to predict prognosis, immune landscape, and chemotherapy response in colon adenocarcinoma. Front Immunol. 2022;13:1038927.
53. Biswas SK, Allavena P, Mantovani A. Tumor-associated macrophages: functional diversity, clinical significance, and open questions. Semin Immunopathol. 2013;35(5):585–600.
54. Badawi MA, Abouelfadl DM, El-Sharkawy SL, El-Aal WE, Abbas NF. Tumor-Associated Macrophage (TAM) and Angiogenesis in Human Colon Carcinoma. Open Access Maced J Med Sci. 2015;3(2):209–14.
55. Yahaya MAF, Lila MAM, Ismail S, Zainol M, Afizan N. Tumour-Associated Macrophages (TAMs) in Colon Cancer and How to Reeducate Them. J Immunol Res. 2019;2019:2368249.
56. Darvin P, Toor SM, Sasidharan Nair V, Elkord E. Immune checkpoint inhibitors: recent progress and potential biomarkers. Exp Mol Med. 2018;50(12):1–11.
57. Kamal AM, Wasfey EF, Elghamry WR, Sabry OM, Elghobary HA, Radwan SM. Genetic signature of CTLA-4, BTLA, TIM-3 and LAG-3 molecular expression in colorectal cancer patients: Implications in diagnosis and survival outcomes. Clin Biochem. 2021;96:13–8.
58. Ma B, Cao L, Li Y. A novel 10-gene immune-related lncRNA signature model for the prognosis of colorectal cancer. Math Biosci Eng. 2021;18(6):9743–60.
59. Gao HL, Gupta P, Cui Q, Ashar YV, Wu ZX, Zeng L, et al. Sapitinib Reverses Anticancer Drug Resistance in Colon Cancer Cells Overexpressing the ABCB1 Transporter. Front Oncol. 2020;10: 574861.
60. Razali NN, Raja Ali RA, Muhammad Nawawi KN, Yahaya A, Mohd Rathi ND, Mokhtar NM. Roles of phosphatidylinositol-3-kinases signaling pathway in inflammation-related cancer: Impact of rs10889677 variant and buparlisib in colitis-associated cancer. World J Gastroenterol. 2023;29(40):5543–56.
61. Guan SS, Chang J, Cheng CC, Luo TY, Ho AS, Wang CC, et al. Afatinib and its encapsulated polymeric micelles inhibits HER2-overexpressed colorectal tumor cell growth in vitro and in vivo. Oncotarget. 2014;5(13):4868–80.
62. Gao L, Tian Y, Chen E. The construction of a multi-gene risk model for colon cancer prognosis and drug treatments prediction. Int J Mol Sci. 2024;25(7):3954.
63. Sun S, Huang X, Li G, Zhang C, Lu Z, Zhang W, et al. MACC1 knockdown enhances RSL3-induced ferroptosis in human colorectal cancer cells by inhibiting GPX4 expression. Nan Fang Yi Ke Da Xue Xue Bao. 2024;44(1):173–8.
64. Wang C, Guo J, Zhang Y, Zhou S, Jiang B. Cuproptosis-related gene FDX1 suppresses the growth and progression of colorectal cancer by retarding EMT progress. Biochem Genet. 2024;63(1):775–88.
65. Yang W, Wang Y, Huang Y, Yu J, Wang T, Li C, et al. 4-Octyl itaconate inhibits aerobic glycolysis by targeting GAPDH to promote cuproptosis in colorectal cancer. Biomed Pharmacother. 2023;159: 114301.
66. Chen W, Deng J, Zhou Y. The construction of a novel ferroptosis-related lncRNA model to predict prognosis in colorectal cancer patients. Medicine (Baltimore). 2023;102(10): e33114.
67. Guo Y, Wang Z, Tian Y, Li L, Dong J. A ferroptosis-related lncRNAs signature predicts prognosis of colon adenocarcinoma. Life (Basel). 2023;13(7):1557.

Publisher's Note